the phenotype we observed. However, our results with IL-17$^{-/-}$ CD4$^+$ T cells demonstrated that IL-17 was dispensable for CD4$^+$ T cell-mediated GVHD, indicating that the attenuated GVHD in recipients of IL-21R$^{-/-}$ CD4$^+$ T cells was not due to an IL-17–related defect. During the preparation of this manuscript, a role for IL-17 in GVHD was reported (38–40). These reports varied, but one suggested that the lack of IL-17 promotes GVHD (38). Another report suggested that IL-17$^{-/-}$ CD4$^+$ T cells can ameliorate GVHD only at the early stages, which suggested a promoting effect for IL-17 at an early stage of GVHD (39). The third report suggested that ex vivo-differentiated Th17 cells induced skin and lung GVHD (40). Thus, the role of IL-17 may be complex and dependent on the specific experimental conditions.

Because there are reciprocal relationships between Th1/Th2 and Treg cell differentiation (41–43) and between IL-21 and Treg cell differentiation (8), we investigated the level of Treg cells in the spleens of recipients. Foxp3$^+$CD4$^+$ T cells were increased in percentage and absolute number but still represented only ~1% of splenocytes. Regarding the relationship between the defective effector T cell function and the increased number of Treg cells, it is possible that increased Treg cells suppress functional effector T cells. Alternatively, it is possible that effector differentiation itself is defective, and the resulting effector T cells cannot respond to alloantigen, analogous to the situation in T cell anergy, and that the increased Treg cell number is also a result of a dysregulated differentiation. Our results might be more consistent with the latter possibility, given that Treg cell depletion by anti-CD25 treatment did not alter the results in vitro and in vivo, although the efficiency of depletion of Foxp3$^+$CD4$^+$ T cells in vivo was incomplete. It is also conceivable that the upregulation of Foxp3 in CD25$^-$CD4$^+$ T cells (which would not be removed by CD25$^+$ depletion) in the absence of IL-21 signaling might result in unresponsiveness or poor responsiveness of effector T cells and that more than one mechanism can contribute to the attenuated GVHD.

Disclosures

K. Ozaki and W.J.L. are inventors on patents and patent applications related to IL-21.

References

1. Parrish-Novak, J., S. R. Dillon, A. Nelson, A. Hammond, C. Sprecher, J. A. Gross, J. Johnston, K. Madden, W. Xu, J. West, et al. 2000. Interleukin 21 and its receptor are involved in NK cell expansion and regulation of lymphocyte function. *Nature* 408: 57–63.
2. Spolski, R., and W. J. Leonard. 2008. Interleukin-21: basic biology and implications for cancer and autoimmunity. *Annu. Rev. Immunol.* 26: 57–79.
3. Ozaki, K., K. Kikly, D. Michalovich, P. R. Young, and W. J. Leonard. 2000. Cloning of a type I cytokine receptor most related to the IL-2 receptor beta chain. *Proc. Natl. Acad. Sci. USA* 97: 11439–11444.
4. Brandt, K., S. Bulfone-Paus, D. C. Foster, and R. Rückert. 2003. Interleukin-21 inhibits dendritic cell activation and maturation. *Blood* 102: 4090–4098.
5. Ozaki, K., A. Hishiya, K. Hatanaka, H. Nakajima, G. Wang, P. Hwu, T. Kitamura, K. Ozawa, W. J. Leonard, and T. Nosaka. 2006. Overexpression of interleukin 21 induces expansion of hematopoietic progenitor cells. *Int. J. Hematol.* 84: 224–230.
6. Ozaki, K., R. Spolski, C. G. Feng, C. F. Qi, J. Cheng, A. Sher, H. C. Morse, 3rd, C. Liu, P. L. Schwartzberg, and W. J. Leonard. 2002. A critical role for IL-21 in regulating immunoglobulin production. *Science* 298: 1630–1634.
7. Zhou, L., I. I. Ivanov, R. Spolski, R. Min, K. Shenderov, T. Egawa, D. E. Levy, W. J. Leonard, and D. R. Littman. 2007. IL-6 programs T(H)-17 cell differentiation by promoting sequential engagement of the IL-21 and IL-23 pathways. *Nat. Immunol.* 8: 967–974.
8. Nurieva, R., X. O. Yang, G. Martinez, Y. Zhang, A. D. Panopoulos, L. Ma, K. Schluns, Q. Tian, S. S. Watowich, A. M. Jetten, and C. Dong. 2007. Essential autocrine regulation by IL-21 in the generation of inflammatory T cells. *Nature* 448: 480–483.
9. Korn, T., E. Bettelli, W. Gao, A. Awasthi, A. Jäger, T. B. Strom, M. Oukka, and V. K. Kuchroo. 2007. IL-21 initiates an alternative pathway to induce proinflammatory T(H)17 cells. *Nature* 448: 484–487.
10. Wurster, A. L., V. L. Rodgers, A. R. Satoskar, M. J. Whitters, D. A. Young, M. Collins, and M. J. Grusby. 2002. Interleukin 21 is a T helper (Th) cell 2 cytokine that specifically inhibits the differentiation of naive Th cells into interferon gamma-producing Th1 cells. *J. Exp. Med.* 196: 969–977.
11. Pesce, J., M. Kaviratne, T. R. Ramalingam, R. W. Thompson, J. F. Urban, Jr., A. W. Cheever, D. A. Young, M. Collins, M. J. Grusby, and T. A. Wynn. 2006. The IL-21 receptor augments Th2 effector function and alternative macrophage activation. *J. Clin. Invest.* 116: 2044–2055.
12. Fröhlich, A., B. J. Marsland, I. Sonderegger, M. Kurrer, M. R. Hodge, N. L. Harris, and M. Kopf. 2007. IL-21 receptor signaling is integral to the development of Th2 effector responses in vivo. *Blood* 109: 2023–2031.
13. Strengell, M., T. Sareneva, D. Foster, I. Julkunen, and S. Matikainen. 2002. IL-21 up-regulates the expression of genes associated with innate immunity and Th1 response. *J. Immunol.* 169: 3600–3605.
14. Coquet, J. M., S. Chakravarti, M. J. Smyth, and D. I. Godfrey. 2008. Cutting edge: IL-21 is not essential for Th17 differentiation or experimental autoimmune encephalomyelitis. *J. Immunol.* 180: 7097–7101.
15. Sonderegger, I., J. Kisielow, R. Meier, C. King, and M. Kopf. 2008. IL-21 and IL-21R are not required for development of Th17 cells and autoimmunity in vivo. *Eur. J. Immunol.* 38: 1833–1838.
16. Ozaki, K., R. Spolski, R. Ettinger, H. P. Kim, G. Wang, C. F. Qi, P. Hwu, D. J. Shaffer, S. Akilesh, D. C. Roopenian, et al. 2004. Regulation of B cell differentiation and plasma cell generation by IL-21, a novel inducer of Blimp-1 and Bcl-6. *J. Immunol.* 173: 5361–5371.
17. Bubier, J. A., T. J. Sproule, O. Foreman, R. Spolski, D. J. Shaffer, H. C. Morse 3rd, W. J. Leonard, and D. C. Roopenian. 2009. A critical role for IL-21 receptor signaling in the pathogenesis of systemic lupus erythematosus in BXSB- Yaa mice. *Proc. Natl. Acad. Sci. U S A* 106: 1518–1523.
18. King, C., A. Ilic, K. Koelsch, and N. Sarvetnick. 2004. Homeostatic expansion of T cells during immune insufficiency generates autoimmunity. *Cell* 117: 265–277.
19. Spolski, R., M. Kashyap, C. Robinson, Z. Yu, and W. J. Leonard. 2008. IL-21 signaling is critical for the development of type I diabetes in the NOD mouse. *Proc. Natl. Acad. Sci. USA* 105: 14028–14033.
20. Sutherland, A. P., T. Van Belle, A. L. Wurster, A. Suto, M. Michaud, D. Zhang, M. J. Grusby, and M. von Herrath. 2009. Interleukin-21 is required for the development of type 1 diabetes in NOD mice. *Diabetes* 58: 1144–1155.
21. Shlomchik, W. D. 2007. Graft-versus-host disease. *Nat. Rev. Immunol.* 7: 340–352.
22. Meguro, A., K. Ozaki, I. Oh, K. Hatanaka, and H. Matsu, RTatara, K. Sato, W. J. Leonard, and K. Ozawa. 2010. IL-21 is critical for GVHD in a mouse model. *Bone Marrow Transplant.* 45: 723–729.
23. Nakae, S., Y. Komiyama, A. Nambu, K. Sudo, M. Iwase, I. Homma, K. Sekikawa, M. Asano, and Y. Iwakura. 2002. Antigen-specific T cell sensitization is impaired in IL-17-deficient mice, causing suppression of allergic cellular and humoral responses. *Immunity* 17: 375–387.
24. Sakoda, Y., D. Hashimoto, S. Asakura, K. Takeuchi, M. Harada, M. Tanimoto, and T. Teshima. 2007. Donor-derived thymic-dependent T cells cause chronic graft-versus-host disease. *Blood* 109: 1756–1764.
25. Aoyama, K., M. Koyama, K. Matsuoka, D. Hashimoto, T. Ichinohe, M. Harada, K. Akashi, M. Tanimoto, and T. Teshima. 2009. Improved outcome of allogeneic bone marrow transplantation due to breastfeeding-induced tolerance to maternal antigens. *Blood* 113: 1829–1833.
26. Teshima, T., G. R. Hill, L. Pan, Y. S. Brinson, M. R. van den Brink, K. R. Cooke, and J. L. Ferrara. 1999. IL-11 separates graft-versus-leukemia effects from graft-versus-host disease after bone marrow transplantation. *J. Clin. Invest.* 104: 317–325.
27. Beilhack, A., S. Schulz, J. Baker, G. F. Beilhack, C. B. Wieland, E. I. Herman, E. M. Baker, Y. A. Cao, C. H. Contag, and R. S. Negrin. 2005. In vivo analyses of early events in acute graft-versus-host disease reveal sequential infiltration of T-cell subsets. *Blood* 106: 1113–1122.
28. Sakaguchi, S., T. Yamaguchi, T. Nomura, and M. Ono. 2008. Regulatory T cells and immune tolerance. *Cell* 133: 775–787.
29. Sakaguchi, S., N. Sakaguchi, M. Asano, M. Itoh, and M. Toda. 1995. Immunologic self-tolerance maintained by activated T cells expressing IL-2 receptor alpha-chains (CD25). Breakdown of a single mechanism of self-tolerance causes various autoimmune diseases. *J. Immunol.* 155: 1151–1164.
30. Liesz, A., E. Suri-Payer, C. Veltkamp, H. Doerr, C. Sommer, S. Rivest, T. Giese, and R. Veltkamp. 2009. Regulatory T cells are key cerebroprotective immunomodulators in acute experimental stroke. *Nat. Med.* 15: 192–199.
31. Fujita, S., Y. Sato, K. Sato, K. Eizumi, T. Fukaya, M. Kubo, N. Yamashita, and K. Sato. 2007. Regulatory dendritic cells protect against cutaneous chronic graft-versus-host disease mediated through CD4+CD25+Foxp3+ regulatory T cells. *Blood* 110: 3793–3803.
32. Radojcic, V., M. A. Pletneva, H. R. Yen, S. Ivcevic, A. Panoskaltsis-Mortari, A. C. Gilliam, C. G. Drake, B. R. Blazar, and L. Luznik. 2010. STAT3 signaling in CD4+ T cells is critical for the pathogenesis of chronic sclerodermatous graft-versus-host disease in a murine model. *J. Immunol.* 184: 764–774.
33. Yang, Y. G., B. R. Dey, J. J. Sergio, D. A. Pearson, and M. Sykes. 1998. Donor-derived interferon gamma is required for inhibition of acute graft-versus-host disease by interleukin 12. *J. Clin. Invest.* 102: 2126–2135.
34. Murphy, W. J., L. A. Welniak, D. D. Taub, R. H. Wiltrout, P. A. Taylor, D. A. Vallera, M. Kopf, H. Young, D. L. Longo, and B. R. Blazar. 1998. Differential effects of the absence of interferon-gamma and IL-4 in acute graft-versus-host disease after allogeneic bone marrow transplantation in mice. *J. Clin. Invest.* 102: 1742–1748.
35. Wang, H., W. Asavaroengchai, B. Y. Yeap, M. G. Wang, S. Wang, M. Sykes, and Y. G. Yang. 2009. Paradoxical effects of IFN-gamma in graft-versus-host disease reflect promotion of lymphohematopoietic graft-versus-host reactions and inhibition of epithelial tissue injury. *Blood* 113: 3612–3619.
36. Nikolic, B., S. Lee, R. T. Bronson, M. J. Grusby, and M. Sykes. 2000. Th1 and Th2 mediate acute graft-versus-host disease, each with distinct end-organ targets. *J. Clin. Invest.* 105: 1289–1298.

37. Schmaltz, C., O. Alpdogan, S. J. Muriglan, B. J. Kappel, J. A. Rotolo, E. T. Ricchetti, A. S. Greenberg, L. M. Willis, G. F. Murphy, J. M. Crawford, and M. R. van den Brink. 2003. Donor T cell-derived TNF is required for graft-versus-host disease and graft-versus-tumor activity after bone marrow transplantation. *Blood* 101: 2440–2445.
38. Yi, T., D. Zhao, C. L. Lin, C. Zhang, Y. Chen, I. Todorov, T. LeBon, F. Kandeel, S. Forman, and D. Zeng. 2008. Absence of donor Th17 leads to augmented Th1 differentiation and exacerbated acute graft-versus-host disease. *Blood* 112: 2101–2110.
39. Kappel, L. W., G. L. Goldberg, C. G. King, D. Y. Suh, O. M. Smith, C. Ligh, A. M. Holland, J. Grubin, N. M. Mark, C. Liu, et al. 2009. IL-17 contributes to CD4-mediated graft-versus-host disease. *Blood* 113: 945–952.
40. Carlson, M. J., M. L. West, J. M. Coghill, A. Panoskaltsis-Mortari, B. R. Blazar, and J. S. Serody. 2009. In vitro-differentiated TH17 cells mediate lethal acute graft-versus-host disease with severe cutaneous and pulmonary pathologic manifestations. *Blood* 113: 1365–1374.
41. Wei, J., O. Duramad, O. A. Perng, S. L. Reiner, Y. J. Liu, and F. X. Qin. 2007. Antagonistic nature of T helper 1/2 developmental programs in opposing peripheral induction of Foxp3+ regulatory T cells. *Proc. Natl. Acad. Sci. USA* 104: 18169–18174.
42. Mantel, P. Y., H. Kuipers, O. Boyman, C. Rhyner, N. Ouaked, B. Rückert, C. Karagiannidis, B. N. Lambrecht, R. W. Hendriks, R. Crameri, et al. 2007. GATA3-driven Th2 responses inhibit TGF-beta1-induced FOXP3 expression and the formation of regulatory T cells. *PLoS Biol.* 5: e329.
43. Hill, J. A., J. A. Hall, C. M. Sun, Q. Cai, N. Ghyselinck, P. Chambon, Y. Belkaid, D. Mathis, and C. Benoist. 2008. Retinoic acid enhances Foxp3 induction indirectly by relieving inhibition from CD4+CD44hi Cells. *Immunity* 29: 758–770.

Promotion of direct reprogramming by transformation-deficient Myc

Masato Nakagawa[a,1], Nanako Takizawa[a], Megumi Narita[a,b], Tomoko Ichisaka[a,b], and Shinya Yamanaka[a,b,c,d,1]

[a]Center for iPS Cell Research and Application and [b]Institute for Integrated Cell–Material Sciences, Kyoto University, Kyoto 606-8507, Japan; [c]Yamanaka iPS Cell Special Project, Japan Science and Technology Agency, Kawaguchi 332-0012, Japan; and [d]Gladstone Institute of Cardiovascular Disease, San Francisco, CA 94158

Communicated by Yuet Wai Kan, University of California San Francisco School of Medicine, San Francisco, CA, June 30, 2010 (received for review June 24, 2010)

Induced pluripotent stem cells (iPSCs) are generated from mouse and human fibroblasts by the introduction of three transcription factors: Oct3/4, Sox2, and Klf4. The proto-oncogene product c-Myc markedly promotes iPSC generation, but also increases tumor formation in iPSC-derived chimeric mice. We report that the promotion of iPSC generation by Myc is independent of its transformation property. We found that another Myc family member, L-Myc, as well as c-Myc mutants (W136E and dN2), all of which have little transformation activity, promoted human iPSC generation more efficiently and specifically compared with WT c-Myc. In mice, L-Myc promoted germline transmission, but not tumor formation, in the iPSC-derived chimeric mice. These data demonstrate that different functional moieties of the Myc proto-oncogene products are involved in the transformation and promotion of directed reprogramming.

induced pluripotent stem cell | embryonic stem cell | regenerative medicine | proto-oncogene

Induced pluripotent stem cells (iPSCs) were first generated from mouse fibroblasts by the retroviral introduction of four transcription factors: Oct3/4, Sox2, Klf4, and c-Myc (1). Mouse iPSCs are indistinguishable from embryonic stem cells (ESCs) in morphology, proliferation and gene expression. Furthermore, mouse iPSCs give rise to chimeric mice that are competent for germline transmission (2–4). However, both the chimeras and progenies derived from mouse iPSC have an increased incidence of tumor formation, due primarily to reactivation of the c-Myc retrovirus (3). We and others successfully created mouse iPSCs without the c-Myc retrovirus by modifying the induction protocol (5, 6). Chimeric mice derived from these c-Myc–minus iPSCs did not demonstrate an increased incidence of tumor formation (6). The efficiency of iPSC generation is significantly lower without the c-Myc retrovirus, however. Indeed, c-Myc is used in most of the reported methods to generate iPSCs without viral integration (7–15). Thus, c-Myc functions as a "double-edged sword," promoting both iPSC generation and tumorigenicity.

In addition to the overexpression of c-Myc, we and others have shown that suppression of the tumor-suppressor gene p53 also significantly enhances iPSC generation (16–19). The downstream targets of p53, including p21 and Arf/Ink4, also are involved in the suppression of iPSC generation. The fact that the two most common pathways associated with human cancers—activation of c-Myc and suppression of p53—both substantially enhance iPSC generation raises the possibility that the molecular mechanisms underlying iPSC generation and tumorigenicity largely overlap.

The Myc proto-oncogene family consists of three members: c-Myc, N-Myc, and L-Myc (20–23). All three members dimerize with Max and binding to DNA (24). N-Myc is similar to c-Myc in terms of length, domain structures, and frequent association with human cancers (25). In contrast, the L-Myc protein has shorter amino acid sequences than the other two members in the N-terminal region, along with significantly lower transformation activity in cultured cells (21, 26–29). Consistent with this property, only a small number of human cancers have been associated with the aberrant expression of L-Myc. In the present study, we analyzed the effect of L-Myc in promoting iPSC generation. Despite its weak transformation activity, L-Myc was found to have a stronger and more specific activity in promoting iPSC generation. In addtion, the mutations that significantly deteriorate the transformation activity of c-Myc more effectively and specifically promote human iPSC generation. These findings demonstrate that the promotion of nuclear-reprogramming and transformation activity are independent properties of the Myc family proteins.

Results

To compare the effects of L-Myc, N-Myc, and c-Myc on human iPSC generation, we retrovirally transduced human adult dermal fibroblasts with Oct3/4, Sox2, and Klf4, with or without the Myc family members. Then, 3 wk later, we counted the numbers of both iPSC colonies, which had an ESC-like morphology with a flat, round shape and a distinct edge, and non-iPSC colonies, which were granulous with an irregular edge. Compared with c-Myc, L-Myc demonstrated significantly more potency in increasing the number of iPSC colonies (Fig. 1*A*). N-Myc also tended to increase the iPSC colonies more effectively compared with c-Myc, although the difference was not statistically significant. We also found that c-Myc and N-Myc markedly increased the formation of non-iPSC colonies, whereas L-Myc did not. As a result, the proportion of iPSC colonies out of the total colonies is significantly higher with L-Myc than with c-Myc or N-Myc (Fig. 1*B*).

Human iPSCs generated with L-Myc showed a morphology similar to that of human ESCs (Fig. 1*C*). They were positive for various pluripotent markers, including Tra-1–60, Tra-1–81, SSEA-3, and Oct3/4 (Fig. S1*A*). They differentiated into various tissues of three germ layers, including neural tissues, gut-like epithelial cells, cartilage, and adipose tissue, in teratomas (Fig. S1*B*) and in embryoid bodies (Fig. S1*C*). They had normal karyotypes (Fig. S1*D*). These findings indicate that L-Myc promotes human iPSC generation more specifically and effectively compared with c-Myc.

We next compared the three Myc members in terms of mouse iPSC generation. Mouse embryonic fibroblasts (MEFs), which have a GFP reporter driven by the regulatory regions of the mouse *Nanog* gene, were retrovirally transduced with Oct3/4, Sox2, and Klf4 with or without each of the Myc family members. After 3 wk, the numbers of GFP-positive and GFP-negative colonies were counted. GFP-positive colonies represent fully reprogrammed iPSCs, whereas GFP-negative colonies represent partially reprogrammed or transformed cells. As reported previously (6), all three Myc proteins enhanced the generation of GFP-positive colonies (Fig. 2*A*). c-Myc had a stronger effect than the other two Myc proteins, but its effects

Author contributions: M. Nakagawa and S.Y. designed research; M. Nakagawa, N.T., M. Narita, and T.I. performed research; M. Nakagawa contributed new reagents/analytic tools; M. Nakagawa analyzed data; and M. Nakagawa and S.Y. wrote the paper.

The authors declare no conflict of interest.

[1]To whom correspondence may be addressed. E-mail: nakagawa@cira.kyoto-u.ac.jp or yamanaka@cira.kyoto-u.ac.jp.

This article contains supporting information online at www.pnas.org/lookup/suppl/doi:10.1073/pnas.1009374107/-/DCSupplemental.

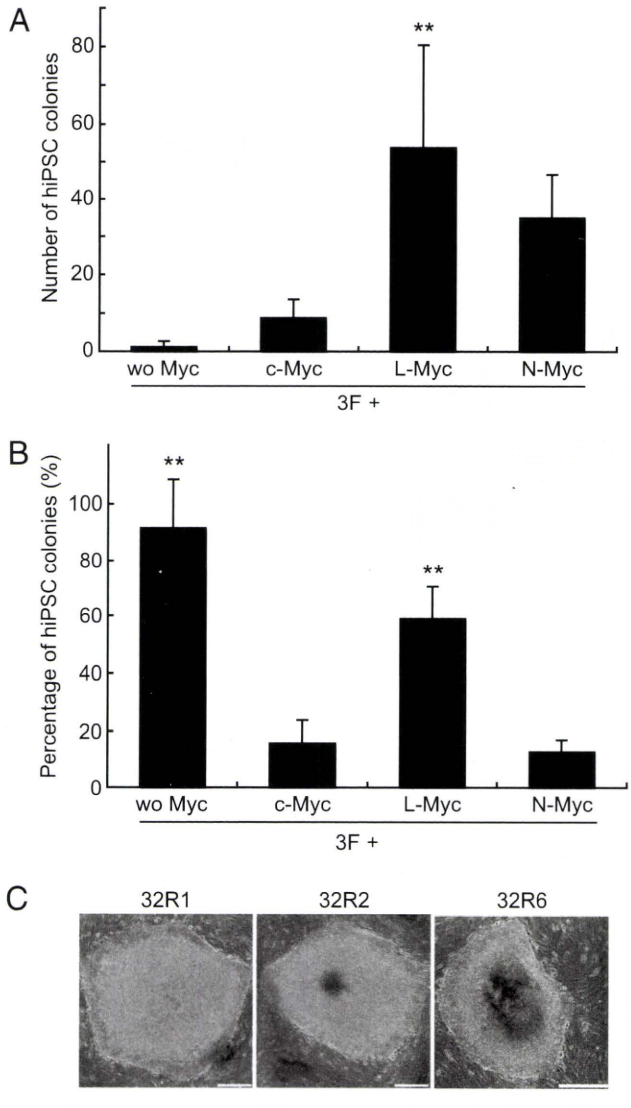

Fig. 1. Promotion of human iPSC generation by L-Myc. (*A*) The number of human iPSC colonies from aHDFs transduced with or without the indicated Myc family genes ($n = 4$; $^{**}P < 0.01$ vs. without Myc or c-Myc). (*B*) The effect of Myc on the percentage of human iPSC colonies out of all colonies ($n = 4$; $^{**}P < 0.01$ vs. c-Myc or N-Myc). (*C*) Morphology of L-Myc human iPSCs. (Scale bar: 200 μm.)

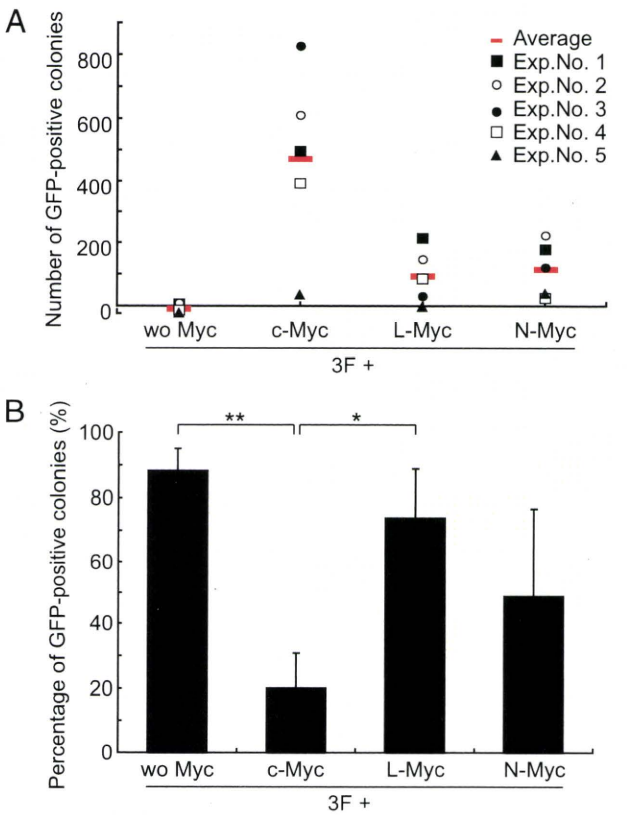

Fig. 2. Generation of mouse iPSCs with L-Myc. (*A*) Generation of mouse iPSCs with or without the indicated Myc family genes from MEFs containing the Nanog-GFP reporter. The raw data from five independent experiments (experiments 1–5) are shown. Each red line shows the average of five experiments in the indicated condition. (*B*) Effect of the Myc family genes on the percentage of GFP-positive colonies out of all colonies ($n = 5$; $^{*}P < 0.05$; $^{**}P < 0.01$).

were more profound on GFP-negative colonies than on GFP-positive colonies, resulting in a significant decrease in the proportion of GFP-positive colonies out of the total colonies (Fig. 2*B*). In contrast, L-Myc preferentially increased GFP-positive colonies, while the proportion of GFP-positive colonies out of the total colonies remained high. These findings demonstrate that L-Myc specifically enhances the generation of fully reprogrammed mouse iPSCs.

Mouse iPSCs generated with L-Myc showed an ESC-like morphology (Fig. S2*A*) and expressed pluripotent-associated genes, including *Nanog*, *Rex1*, *ECAT1*, and *ESG1* (Fig. S2*B*). The expression of retroviral transgenes was effectively silenced. When transplanted subcutaneously into nude nice, these cells formed teratomas containing various tissues, including neural tissues, gut-like epithelial tissues, and striated muscles (Fig. S2*C*). Furthermore, when injected into blastocysts, L-Myc iPSCs were capable of producing high-percentage chimeras that were competent for germline transmission. Of note, both c-Myc and L-Myc promoted germline transmission from chimeras compared with iPSCs generated without the Myc transgenes (Fig. 3*A*). This suggests that iPSCs generated with L-Myc are of a comparable quality to ESCs.

We previously reported that iPSCs generated with the c-Myc retrovirus resulted in a markedly increased tumor formation and mortality in chimeras and progeny mice (3, 30). In contrast, iPSCs generated without the c-Myc transgene did not show any such adverse effects in mice (6). In this study, we observed chimeras derived from L-Myc iPSC clones for up to 2 y. In stark contrast to c-Myc, the L-Myc retrovirus did not result in any marked increase in either tumorigenicity or mortality (Fig. 3*B*). Compared with chimeric mice derived from Myc-minus iPSCs, L-Myc iPSCs exhibited slightly higher mortality, but not tumorigenicity, in mice at 1 y after birth. The causes of death in these mice remain to be determined. These findings are consistent with the weak transformation activity of L-Myc.

We also examined whether L-Myc was capable of decreasing the number of factors required for iPSC generation. We found that with the addition of L-Myc, iPSCs can be generated without Sox2. Infecting 1×10^5 Nanog-GFP reporter MEFs with Oct3/4, Klf4, and L-Myc yielded 16 GFP-positive colonies. In contrast, no GFP-positive colonies were obtained without the L-Myc transgene. We picked up all of these colonies and were able to establish iPSC lines from 15 clones. These Sox2-minus iPSCs showed an ESC-like morphology (Fig. S3*A*) and expressed ESC markers, including *Nanog*, *Rex1*, and *ECAT1* (Fig. S3*B*). We confirmed the absence of the Sox2 transgene by genomic PCR (Fig. S3*C*). These cells can differentiate into cells of three germ layers in teratomas (Fig. S3*D*) and embryoid bodies (Fig. S3*E*). Sox2-minus L-Myc iPSCs were capable of producing chimeras that were competent for germline transmission (Fig. S3*F*).

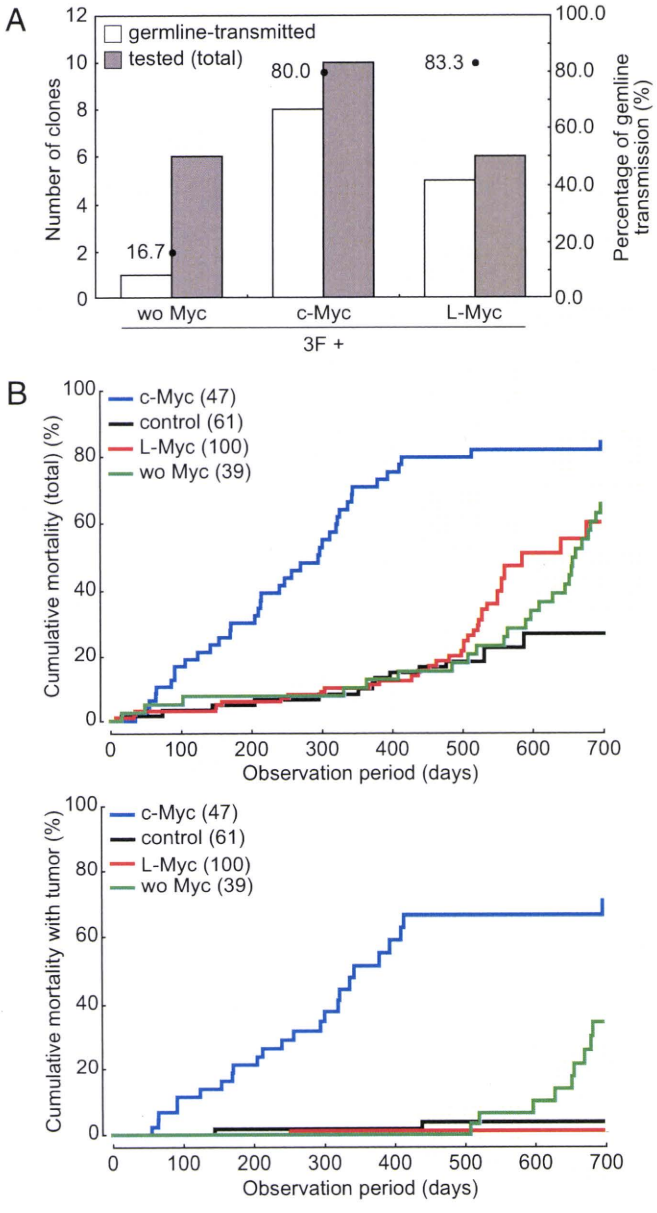

Fig. 3. Chimeric mice derived from L-Myc iPSCs. (*A*) Frequency of germline transmission of mouse iPSC clones established without Myc or with either c-Myc or L-Myc. The white columns indicate how many iPSC clones gave rise to germline transmission, and the gray columns indicate how many clones were tested. Also shown are the percentages of germline-competent iPSC clones out of all clones tested. (*B*) The cumulative overall mortality (*Upper*) and morality with microscopically obvious tumors (*Lower*) in the chimeric mice derived from iPSCs with c-Myc or L-Myc. The numbers in parentheses refer to the total number of animals tested in each group.

We next examined the correlation between the ability to promote iPSC generation and the transformation activity of the Myc proteins. We constructed the W136E c-Myc mutant, which reportedly lacks transformation activity but still binds to Max and DNA (26, 31). We also generated a mutant of c-Myc that does not bind to Miz-1 (V394D) (32) and other mutants of c-Myc and L-Myc that do not bind to Max (c-Myc L420P and L-Myc L351P) (33). The WT L-Myc, the W136E c-Myc mutant, the L420P c-Myc mutant, and the L351P L-Myc mutant showed little transformation activity in NIH 3T3 cells (Fig. 4*A*). In contrast, the WT c-Myc– and V394D c-Myc mutant–induced transformation was characterized by high refractivity and a spindle-like shape. We then introduced either the WT or mutant c-Myc into aHDFs together with Oct3/4, Sox2, and Klf4 to generate iPSC colonies. We found that the W136E c-Myc mutant functioned similarly to L-Myc, increasing the number of iPSC colonies more effectively than the WT c-Myc (Fig. 4*B*). In addition, the proportion of iPSC colonies out of the total colonies was higher with the W136E mutant c-Myc than with the WT c-Myc (Fig. S4*A*). The V394D c-Myc mutant was comparable to the WT c-Myc, indicating that the binding to Miz-1 plays neither a positive nor a negative role in the promotion of iPSC generation. The L420P c-Myc or L351P L-Myc mutant did not promote iPSC generation, demonstrating the essential role of Max binding. Similar results were obtained in mice (Fig. S4 *C* and *D*); the W136E c-Myc mutant, like L-Myc, specifically promoted mouse iPSC generation, whereas the V394D c-Myc mutant, like the WT c-Myc, promoted both iPSC and non-iPSC generation.

We also constructed c-Myc mutants with a shorter N terminus, designated dN1 and dN2. The c-Myc protein was ~22 amino acids longer than L-Myc in the N terminus. These extra amino acids were deleted in the dN2 mutant, whereas only 14 amino acids were deleted in the dN1 mutant. The dN2 mutant showed little transformation activity in NIH 3T3 cells, whereas the dN1 mutant showed activity comparable to that of the WT c-Myc (Fig. 4*C*). The dN2 mutant had similar properties as the WT L-Myc and the W136E c-Myc mutant during iPSC generation in both humans (Fig. 4*D* and Fig. S4*B*) and mice (Fig. S4 *E* and *F*). In contrast, the dN1 mutant was comparable to the WT c-Myc. Taken together, these data indicate that the promotion of iPSC generation by Myc is not parallel to its transformation activity.

We performed DNA microarray analyses to elucidate the molecular mechanisms underlying the various effects of c-Myc and L-Myc during iPSC generation. We expressed either c-Myc (WT, W136E, V394D, or L420P) or L-Myc (WT or L351P) in aHDFs by retroviruses. At 2 d after transduction, we isolated total RNA for microarray analyses. We categorized genes that were either increased or decreased by >2-fold by Myc into four groups: group A, increased >2-fold by WT c-Myc and the V394D c-Myc mutant compared with mock-transduced control (Mock) and the L420P c-Myc mutant; group B, decreased >2-fold by WT c-Myc and the V394D c-Myc mutant compared with Mock and the L420P c-Myc mutant; group C, increased >2-fold by WT L-Myc and the W136E c-Myc mutant compared with Mock and the corresponding Max-biding deficient mutant; and group D, decreased >2-fold by WT L-Myc and the W136E c-Myc mutant compared with Mock and the Max-biding deficient mutant. Groups A and B represent the genes regulated by Myc proteins that promote both iPSC generation and transformation. Groups C and D represent genes regulated by Myc proteins that specifically promote iPSC generation, but not transformation.

We found that c-Myc and L-Myc regulate both common (subgroups AC and BD) and unique (subgroups A, C, B, and D) target genes (Fig. 5*A*). The genes in each subgroup are listed in Dataset S1. Subgroups A and AC are enriched with genes that are highly expressed in human ESCs as well as cancer cells, such as bladder tumors and nasopharyngeal carcinomas (Fig. 5 *B* and *C*). The increased expression of these genes might be associated with the transformation activity of Myc. In contrast, subgroups BD and D are enriched with genes that are highly expressed in fibroblasts, but not in ESCs or iPSCs. This result suggests that the promotion of iPSC generation by Myc might be associated with the suppression of fibroblast-specific genes, and that L-Myc is more potent than c-Myc in this specific gene regulatory function.

Discussion

In this study, we found that among the three Myc family proteins c-Myc, N-Myc, and L-Myc, L-Myc showed the strongest and most specific activity in promoting human iPSC generation. This finding was surprising, given that L-Myc has been shown to have

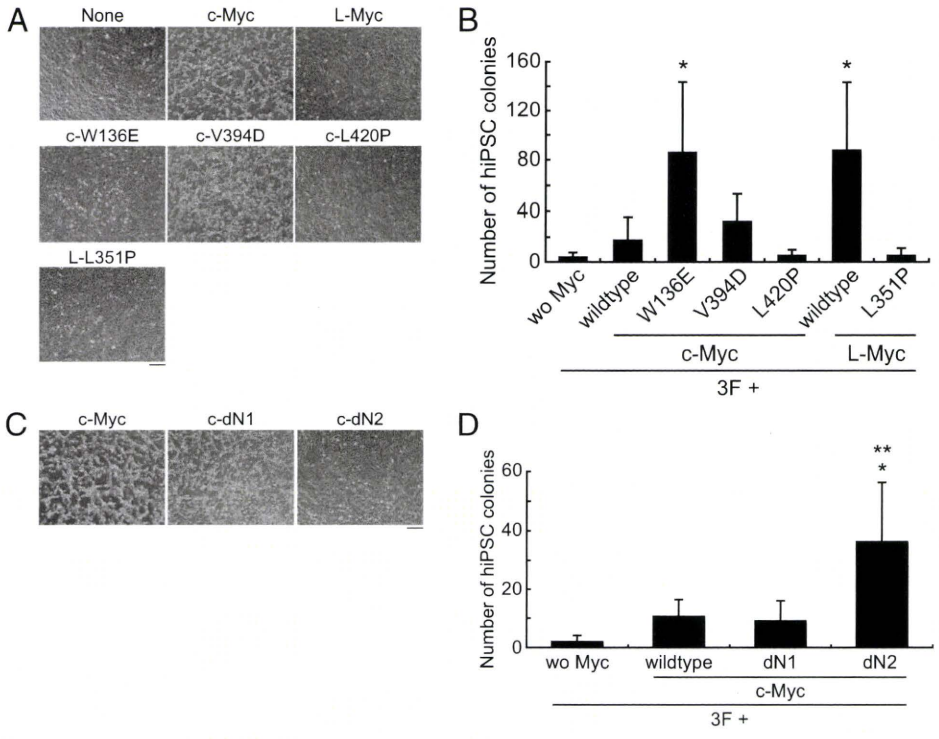

Fig. 4. Promotion of iPSC generation by transformation-deficient Myc mutants. (*A*) Transformation activity of WT and mutant Myc in NIH 3T3 cells. (Scale bar: 100 μm.) (*B*) Generation of human iPSCs with Myc mutants. The numbers of human iPSC colonies are shown (n = 9; *P < 0.05 vs. WT c-Myc). (*C*) Transformation activity of N-terminus deleted c-Myc mutants in NIH 3T3 cells. (Scale bar: 100 μm.) (*D*) Generation of human iPSCs by N-terminus deleted c-Myc mutants. The numbers of human iPSC colonies are shown (n = 3; *P < 0.05 vs. WT or dN1 c-Myc; **P < 0.01 vs. without Myc).

the weakest transformation activity among the three proteins (21, 25, 26, 28). We also found that the mutations that deteriorate the transformation activity of c-Myc specifically promote iPSC generation. Our findings demonstrate that iPSC generation and transformation use different functional moieties of the Myc proto-oncogene products.

Our DNA microarray analyses suggest that L-Myc and the transformation-deficient W136E c-Myc mutant have different target genes than those of the WT c-Myc. When overexpressed in aHDFs, L-Myc and the W136E c-Myc mutant suppressed numerous genes that are highly expressed in fibroblasts compared with iPSCs or ESCs. In contrast, only a small number of genes were selectively activated by L-Myc and the W136E c-Myc. Thus, we postulate that the primary role of these Myc proteins in promoting iPSC generation might be to suppress differentiation-associated genes. This finding is consistent with a previous report on c-Myc (34), and we also found that both L-Myc and the W136E c-Myc mutant were more potent than the WT c-Myc.

Our DNA microarray analyses also revealed that the WT c-Myc protein activated many genes that were enriched not only in ESCs and iPSCs, but also in cancer cells. These gene products might be associated with cell proliferation, immortality, and cell metabolism. Approximately half of these were specifically activated by the WT c-Myc, but not by L-Myc or the W136E c-Myc mutant. These genes are might be responsible, at least in part, for the transformation activity of c-Myc.

We found that the effects of L-Myc and the transformation-deficient mutants of c-Myc in enhancing iPSC generation were more potent in humans than in mice. The reasons for this difference remain to be determined. This finding suggests that the molecular mechanisms underlying iPSC generation might be similar, but not identical, in humans and mice.

Since its first demonstration in 2006, iPSC generation has been associated with transformation and tumorigenicity (1). All four of the factors required for iPSC generation have been associated with human cancers. The most obvious example is c-Myc, one of the first proto-oncogenes identified in human cancers (35). Aberrant expression of c-Myc is found in >50% of human cancers. Klf4 plays a unique role in cancer, functioning as both a proto-oncogene and a tumor-suppressor gene (36). Klf4 promotes cellular transformation by suppressing p53, but it also enhances the activity of p21 and thus may function as a tumor suppressor depending on the cellular context (37). Aberrant expression of Oct3/4 and Sox2 also has been found in some germ cell tumors and other tumors (38–42).

The association of iPSC generation and transformation is demonstrated by the increased incidence of tumor formation observed in chimeric mice derived from iPSCs (3, 30). More than 50% of chimeras derived from MEF-derived four factor–induced iPSC were found to develop tumors within 1 y after birth. Reactivation of the c-Myc retrovirus was detected in these tumors. In contrast, chimeras derived from iPSCs generated without the c-Myc retrovirus showed no increased incidence of tumorigenicity (6). Thus, c-Myc seems to play a major role in the observed tumorigenicity in iPSC-derived mice.

More recently, multiple groups have independently reported that suppression of the tumor-suppressor gene p53 markedly enhances iPSC generation (16–19). The loss of p53 functions, such as the aberrant expression of c-Myc, has been associated with numerous human tumors (43–47). Taken together, these findings indicate that iPSC generation and cellular transformation have many molecular mechanisms and pathways in common, and thus increasing the efficacy of iPSC generation can be achieved at the expense of increased tumor formation.

In contrast to these predictions, our data show that iPSC generation and transformation by Myc are largely independent

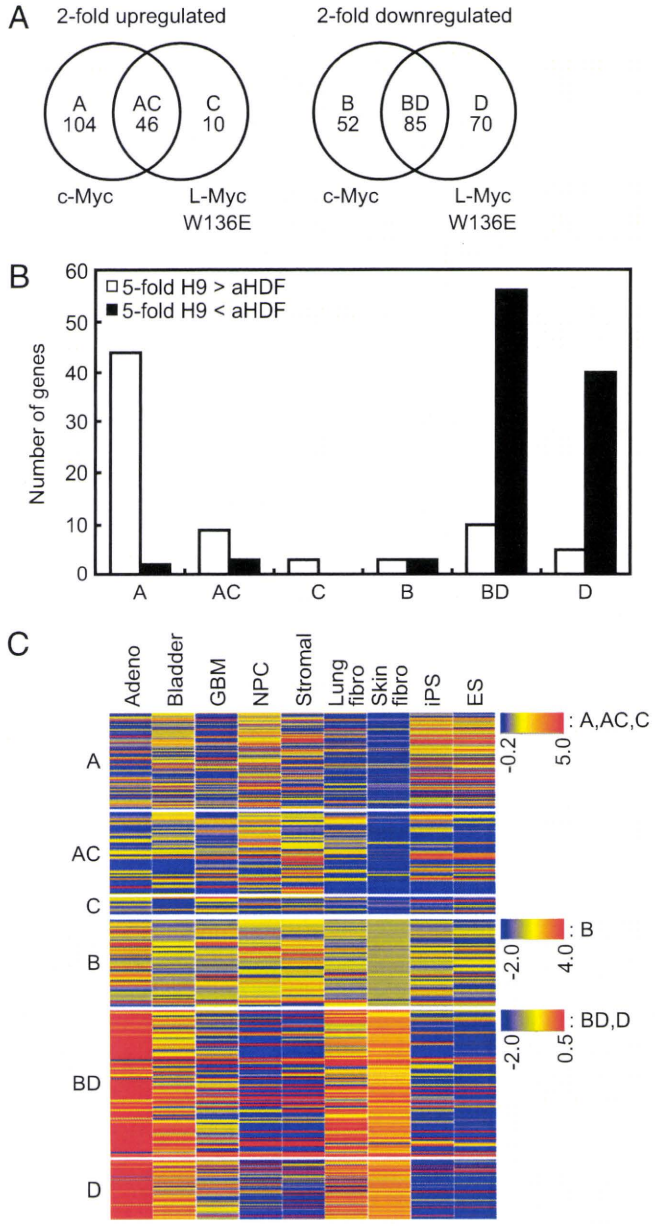

Fig. 5. Genes regulated by Myc proteins. (*A*) Subgroups of the genes regulated by Myc proteins. Venn diagrams were constructed from groups A, B, C, and D. The numbers of the genes in each list are shown; these genes are listed in Dataset S1. (*B*) Regulation of aHDF- or ESC-enriched genes by Myc. Shown is the number of genes with expression >5-fold higher or lower in hESCs (H9) than in aHDFs in each subgroup. (*C*) Comparison of gene expression in cancer cells, normal fibroblasts, iPSCs, and ESCs. Shown are the expression levels of the genes in each subgroup in five cancer cells, two normal fibroblasts, human iPSCs (average of three clones: 201B2, 201B7, and 253G1), and human ESCs (average of four clones: H1, H9, KhES1, and KhES3). Adeno, adenocarcinomas; bladder, bladder cancer; GBM, glioblastoma; NPC, nasopharyngeal carcinoma; stromal, stromal tumor; lung fibro, normal lung fibroblasts.

processes. The former is attributable mainly to the suppression of genes that are highly expressed in fibroblasts, but not in iPSCs or ESCs. In contrast, transformation is attributable to the activation of genes that are enriched in highly proliferative cells, including cancer cells, iPSCs and ESCs. Although methods of iPSC generation that do not result in permanent integration of transgenes have been reported (7–15), even transient expression of the c-Myc transgene might have detrimental effects on the resulting iPSCs. Thus, the use of L-Myc or transformation-deficient mutants of c-Myc should be beneficial for future clinical applications of iPSC technologies.

Materials and Methods

Construction of Plasmids. The pMXs-based retroviral vectors for mouse Myc family genes have been described previously (6). The coding regions of human L-Myc and N-Myc were amplified by RT-PCR with the primers listed in Table S1. N-terminus deleted c-Myc mutants (cdN1, 14–439 aa; cdN2, 42–439 aa) were amplified by the PCR primers listed in Table S2. These PCR products were subcloned into pENTR-D-TOPO (Invitrogen) and then recombined with pMXs-gw via the LR reaction (Invitrogen). For the construction of Myc point mutants, site-directed mutagenesis was performed using PrimeSTAR HS DNA Polymerase (TaKaRa) with the primers listed in Table S3, according to the manufacturer's instructions.

Generation of iPSCs. Induction of mouse iPSCs was performed as described previously (1, 3, 6) with some modifications. In brief, MEFs containing the Nanog-GFP-IRES-Puro^r reporter were seeded in six-well plates at 1.0×10^5 cells/well. The next day (day 0), the cells were infected with retorvirsuses containing three or four factors. On day 3, the cells were replated onto mitomycin C–treated SNL feeder cells (48). The transduced cells were cultivated with ES medium containing leukemia inhibitory factor (49). Selection with puromycin (1.5 μg/mL) was started on day 21. Between 25 and 30 d after transduction, the number of colonies was manually counted under a microscope and recorded. Some colonies were then selected for expansion. The induction of human iPSCs was performed as described previously (6, 50). Adult human dermal fibroblasts (aHDFs) from the facial dermis of a 36-y-old Caucasian female were purchased from Cell Applications.

RNA Isolation and Reverse-Transcription. The purifications of total RNA and RT-PCR were performed as described previously (1, 3, 6, 50). The expression of L-Myc was detected with a primer set, as listed in Table S4.

Transformation Assay in NIH 3T3 Cells. NIH 3T3 cells were plated in 24-well plates at 2.5×10^4 cells/well. The next day, the cells were infected with WT or mutant Myc. Two days after infection, the transfomation activity was determined based on the morphological changes detected.

DNA Microarray Analyses. A DNA microarray analysis was performed as described previously (50). First, aHDFs were retrovirally infected with WT or mutant Myc. Then at 48 hours after infection, total RNA was extracted from the cells and used for microarray experiments (GSE22654). Data were analyzed using the GeneSpring GX 11 software package (Agilent). The genes activated or suppressed by Myc proteins were identified and categorized as described in *Results*. According to the expression levels of these selected genes, hierarchical clustering of the log2 expression ratios was performed for five cancer cells, two normal cells (aHDFs and lung fibroblasts), human iPSCs (average of three clones: 201B2, 201B7, and 253G1), and human ESCs (average of four clones: H1, H9, KhES1, and KhES3). The microarray data for cancer cells and lung fibroblasts were obtained from GEO DataSets (adenocarcinomas, GSE13213; bladder cancer, GSE19716; glioblastoma, GSE10878; nasopharyngeal carcinoma, GSE15191; stromal tumor, GSE17018; lung fibroblasts, GSE15359).

Statistical Analyses. Data are presented as average ± SD. All statistical analyses were performed with one-way repeated-measures ANOVA and the Bonferroni post hoc test, using KaleidaGraph 4 (HULINKS).

ACKNOWLEDGMENTS. We thank Drs. Takashi Aoi, Yoshinori Yoshida, Keisuke Okita, and Kazutoshi Takahashi and other members of Yamanaka research group for scientific comments and valuable discussions; Mika Ohuchi for assistance in the animal experiments; Tokiko Ohkame and Yukari Matsukawa for karyotype analyses; Dr. Toshio Kitamura (The Advanced Clinical Research Center, The Institute of Medical Science, The University of Tokyo, Tokyo) for the retroviral expression system; and Dr. Peter W. Andrews (University of Sheffield, Sheffield, UK) for anti-SSEA-3, Tra-1-60, and Tra-1-81 antibodies. We also thank Rie Kato, Eri Nishikawa, Yuko Ohtsu, Sayaka Takeshima, and Haruka Hasaba for their valuable administrative support. This study was supported in part by a grant from the Program for Promotion of Fundamental Studies in Health Sciences of the National Institute of Biomedical Innovation, a grant from the Leading Project of the Ministry of Education, Culture, Sports, Science and Technology (MEXT), a grant from Funding Program for World-Leading Innovative R&D on Science and Technology (FIRST Program) of the Japan Society for the Promotion of Science (JSPS), and Grants-in-Aid for Scientific Research of JSPS and MEXT.

1. Takahashi K, Yamanaka S (2006) Induction of pluripotent stem cells from mouse embryonic and adult fibroblast cultures by defined factors. *Cell* 126:663–676.
2. Wernig M, et al. (2007) In vitro reprogramming of fibroblasts into a pluripotent ES-cell–like state. *Nature* 448:318–324.
3. Okita K, Ichisaka T, Yamanaka S (2007) Generation of germline-competent induced pluripotent stem cells. *Nature* 448:313–317.
4. Maherali N, et al. (2007) Directly reprogrammed fibroblasts show global epigenetic remodeling and widespread tissue contribution. *Cell Stem Cell* 1:55–70.
5. Wernig M, Meissner A, Cassady JP, Jaenisch R (2008) c-Myc is dispensable for direct reprogramming of mouse fibroblasts. *Cell Stem Cell* 2:10–12.
6. Nakagawa M, et al. (2008) Generation of induced pluripotent stem cells without Myc from mouse and human fibroblasts. *Nat Biotechnol* 26:101–106.
7. Okita K, Nakagawa M, Hyenjong H, Ichisaka T, Yamanaka S (2008) Generation of mouse induced pluripotent stem cells without viral vectors. *Science* 322:949–953.
8. Yusa K, Rad R, Takeda J, Bradley A (2009) Generation of transgene-free induced pluripotent mouse stem cells by the piggyBac transposon. *Nat Methods* 6:363–369.
9. Woltjen K, et al. (2009) piggyBac transposition reprograms fibroblasts to induced pluripotent stem cells. *Nature* 458:766–770.
10. Kim DH, et al. (2009) Generation of human induced pluripotent stem cells by direct delivery of reprogramming proteins. *Cell Stem Cell* 4:472–476.
11. Yu J, et al. (2009) Human induced pluripotent stem cells free of vector and transgene sequences. *Science* 324:797–801.
12. Fusaki N, Ban H, Nishiyama A, Saeki K, Hasegawa M (2009) Efficient induction of transgene-free human pluripotent stem cells using a vector based on Sendai virus, an RNA virus that does not integrate into the host genome. *Proc Jpn Acad Ser B* 85: 348–362.
13. Stadtfeld M, Nagaya M, Utikal J, Weir G, Hochedlinger K (2008) Induced pluripotent stem cells generated without viral integration. *Science* 322:945–949.
14. Zhou W, Freed CR (2009) Adenoviral gene delivery can reprogram human fibroblasts to induced pluripotent stem cells. *Stem Cells* 27:2667–2674.
15. Zhou H, et al. (2009) Generation of induced pluripotent stem cells using recombinant proteins. *Cell Stem Cell* 4:381–384.
16. Marión RM, et al. (2009) A p53-mediated DNA damage response limits reprogramming to ensure iPS cell genomic integrity. *Nature* 460:1149–1153.
17. Kawamura T, et al. (2009) Linking the p53 tumour suppressor pathway to somatic cell reprogramming. *Nature* 460:1140–1144.
18. Hong H, et al. (2009) Suppression of induced pluripotent stem cell generation by the p53-p21 pathway. *Nature* 460:1132–1135.
19. Zhao Y, et al. (2008) Two supporting factors greatly improve the efficiency of human iPSC generation. *Cell Stem Cell* 3:475–479.
20. Cole MD (1986) The myc oncogene: Its role in transformation and differentiation. *Annu Rev Genet* 20:361–384.
21. Birrer MJ, et al. (1988) L-myc cooperates with ras to transform primary rat embryo fibroblasts. *Mol Cell Biol* 8:2668–2673.
22. Schwab M, Varmus HE, Bishop JM (1985) Human N-myc gene contributes to neoplastic transformation of mammalian cells in culture. *Nature* 316:160–162.
23. Yancopoulos GD, et al. (1985) N-myc can cooperate with ras to transform normal cells in culture. *Proc Natl Acad Sci USA* 82:5455–5459.
24. Blackwell TK, et al. (1993) Binding of myc proteins to canonical and noncanonical DNA sequences. *Mol Cell Biol* 13:5216–5224.
25. Malynn BA, et al. (2000) N-myc can functionally replace c-myc in murine development, cellular growth, and differentiation. *Genes Dev* 14:1390–1399.
26. Oster SK, Mao DY, Kennedy J, Penn LZ (2003) Functional analysis of the N-terminal domain of the Myc oncoprotein. *Oncogene* 22:1998–2010.
27. Hatton KS, et al. (1996) Expression and activity of L-Myc in normal mouse development. *Mol Cell Biol* 16:1794–1804.
28. Barrett J, Birrer MJ, Kato GJ, Dosaka-Akita H, Dang CV (1992) Activation domains of L-Myc and c-Myc determine their transforming potencies in rat embryo cells. *Mol Cell Biol* 12:3130–3137.
29. Cole MD, Cowling VH (2008) Transcription-independent functions of MYC: Regulation of translation and DNA replication. *Nat Rev Mol Cell Biol* 9:810–815.
30. Aoi T, et al. (2008) Generation of pluripotent stem cells from adult mouse liver and stomach cells. *Science* 321:699–702.
31. Brough DE, Hofmann TJ, Ellwood KB, Townley RA, Cole MD (1995) An essential domain of the c-myc protein interacts with a nuclear factor that is also required for E1A-mediated transformation. *Mol Cell Biol* 15:1536–1544.
32. Herold S, et al. (2002) Negative regulation of the mammalian UV response by Myc through association with Miz-1. *Mol Cell* 10:509–521.
33. Blackwood EM, Eisenman RN (1991) Max: A helix-loop-helix zipper protein that forms a sequence-specific DNA-binding complex with Myc. *Science* 251:1211–1217.
34. Sridharan R, et al. (2009) Role of the murine reprogramming factors in the induction of pluripotency. *Cell* 136:364–377.
35. Dang CV, et al. (2006) The c-Myc target gene network. *Semin Cancer Biol* 16:253–264.
36. Nandan MO, Yang VW (2009) The role of Krüppel-like factors in the reprogramming of somatic cells to induced pluripotent stem cells. *Histol Histopathol* 24:1343–1355.
37. Rowland BD, Bernards R, Peeper DS (2005) The KLF4 tumour suppressor is a transcriptional repressor of p53 that acts as a context-dependent oncogene. *Nat Cell Biol* 7:1074–1082.
38. de Jong J, Looijenga LH (2006) Stem cell marker OCT3/4 in tumor biology and germ cell tumor diagnostics: History and future. *Crit Rev Oncog* 12:171–203.
39. Liu A, et al. (2010) Diagnostic utility of novel stem cell markers SALL4, OCT4, NANOG, SOX2, UTF1, and TCL1 in primary mediastinal germ cell tumors. *Am J Surg Pathol* 34: 697–706.
40. Maddison P, Thorpe A, Silcocks P, Robertson JF, Chapman CJ (2010) Autoimmunity to SOX2, clinical phenotype and survival in patients with small-cell lung cancer. *Lung Cancer*.
41. Tung CL, et al. (2010) SOX2 modulates alternative splicing in transitional cell carcinoma. *Biochem Biophys Res Commun* 393:420–425.
42. Peng S, Maihle NJ, Huang Y (2010) Pluripotency factors Lin28 and Oct4 identify a sub-population of stem cell–like cells in ovarian cancer. *Oncogene* 29:2153–2159.
43. Vousden KH, Prives C (2009) Blinded by the light: The growing complexity of p53. *Cell* 137:413–431.
44. Hemann MT, et al. (2005) Evasion of the p53 tumour surveillance network by tumour-derived MYC mutants. *Nature* 436:807–811.
45. Chen Z, et al. (2005) Crucial role of p53-dependent cellular senescence in suppression of Pten-deficient tumorigenesis. *Nature* 436:725–730.
46. Beauséjour CM, et al. (2003) Reversal of human cellular senescence: Roles of the p53 and p16 pathways. *EMBO J* 22:4212–4222.
47. Ferbeyre G, et al. (2002) Oncogenic ras and p53 cooperate to induce cellular senescence. *Mol Cell Biol* 22:3497–3508.
48. McMahon AP, Bradley A (1990) The Wnt-1 (int-1) proto-oncogene is required for development of a large region of the mouse brain. *Cell* 62:1073–1085.
49. Meiner VL, et al. (1996) Disruption of the acyl-CoA:cholesterol acyltransferase gene in mice: Evidence suggesting multiple cholesterol esterification enzymes in mammals. *Proc Natl Acad Sci USA* 93:14041–14046.
50. Takahashi K, et al. (2007) Induction of pluripotent stem cells from adult human fibroblasts by defined factors. *Cell* 131:861–872.

J Clin Periodontol 2010; 37: 1088–1099 doi: 10.1111/j.1600-051X.2010.01597.x

Journal of Clinical Periodontology

Validation of human periodontal ligament-derived cells as a reliable source for cytotherapeutic use

Takanori Iwata[1,2], Masayuki Yamato[1], Zheng Zhang[3], Shigeki Mukobata[4], Kaoru Washio[1], Tomohiro Ando[2], Jan Feijen[3], Teruo Okano[1] and Isao Ishikawa[1,2]

[1]Institute of Advanced Biomedical Engineering and Science; [2]Department of Oral and Maxillofacial Surgery, Tokyo Women's Medical University, Tokyo, Japan; [3]Department of Polymer Chemistry and Biomaterials, Institute for Biomedical Technology (BMTI), Faculty of Science and Technology, University of Twente, AE Enschede, The Netherlands; [4]CellSeed Inc., Tokyo, Japan

Iwata T, Yamato M, Zhang Z, Mukobata S, Washio K, Ando T, Feijen J, Okano T, Ishikawa I. Validation of human periodontal ligament-derived cells as a reliable source for cytotherapeutic use. J Clin Periodontol 2010; 37: 1088–1099. doi: 10.1111/j.1600-051X.2010.01597.x.

Abstract

Aim: Periodontal ligament (PDL) is a reliable cell source for periodontal regeneration. In this study, an optimal protocol for the extraction, expansion, and characterization of human PDL (hPDL) cells was examined for clinical trials.

Materials and Methods: hPDL tissues were obtained from 41 surgically extracted teeth and digested with enzymes. Human adipose-derived stem cells (hADSCs), bone marrow-derived mesenchymal stem cells (hBMMSCs), and gingival fibroblasts (hGFs) were used for comparison. For each sample, the proliferative capacity, colony-forming ability, alkaline phosphatase activity, differentiation ability, the cell surface antigens, gene expression, and regenerative potential were examined.

Results: hPDL cells were more successfully extracted with collagenase/dispase [29/30 (96.7%)] than with trypsin/EDTA [8/11 (72.7%)], and exhibited osteogenic potential both in vitro and in vivo. The proliferation of hPDL cells was rapid at a low cell density. hPDL cells frequently differentiated into cementoblastic/osteoblastic lineage (~ 60%). In contrast, their adipogenic and chondrogenic potentials were lower than those of hADSCs and hBMMSCs. Some genes (NCAM1, S100A4, and periostin) were preferentially expressed in hPDL cells compared with those of hBMMSCs and hGFs. Immunohistochemical studies revealed the expressions of S100A4 and periostin in hPDL tissue.

Conclusion: A protocol for the successful cultivation and validation of hPDL cells is proposed for clinical settings.

Key words: cytotherapy; gene expression profile; marker gene; periodontal ligament cells; regenerative medicine; transplantation; validation

Accepted for publication 27 May 2010

Periodontal regeneration, i.e., the formation of new bone and new cementum with supportive periodontal ligament (PDL), has been a challenge in periodontics, and numerous studies have attempted to induce true periodontal regeneration. The key source of periodontal regeneration is the ''PDL tissue'' (Karring et al. 1985). Once PDL tissues are removed from a dental root, ankylosis and root resorption occur (Nyman et al. 1980, Andreasen & Kristerson 1981). Therefore, researchers consider PDL tissue as a responsible source for periodontal regeneration. Based on this concept, selective proliferation of PDL-derived cells has been clinically performed using barrier membranes (Nyman et al. 1982) or enamel matrix proteins (Hammarstrom et al. 1997). In addition, either alone or a combination use of synthesized and biological materials was utilized to enhance periodontal wound healing during surgical procedures. In most cases, however, only limited histological evidence of true regeneration has been demonstrated (Wang et al. 2005, Sculean et al. 2008).

To overcome the limitations of traditional procedures, transplantation of postnatal stem cells has the potential to significantly alter tissue engineering (Bianco & Robey 2001). Several studies have reported that PDL-derived cells possess stem cell-like properties (Seo et al. 2004, Trubiani et al. 2005, Nagatomo et al. 2006, Gay et al. 2007, Coura et al.

Conflict of interest and source of funding statement

The authors declare that they have no conflict of interests.

This research was supported by ''Formation of Innovation Center for Fusion of Advanced Technologies in the Special Coordination Funds for Promoting Science and Technology'' and a Grant-in-Aid for Young Scientists (B) (20791479) from the Ministry of Education, Culture, Sports, Science, and Technology (MEXT) of Japan.

2008, Lindroos et al. 2008, Zhou et al. 2008, Xu et al. 2009). In addition, because PDL tissues have one of the highest metabolic turnover rates in the body (McCulloch & Bordin 1991, Ramakrishnan et al. 1995, Coura et al. 2008), researchers have hypothesized that a highly regenerative population of cells exists in PDL tissues and that they could be a source of cells for the regeneration of various tissues (Coura et al. 2008). Some studies developed PDL cell transplantation in combination with scaffolds and reported successful periodontal regeneration in animal models (Nakahara et al. 2004, Seo et al. 2004, Sonoyama et al. 2006, Liu et al. 2008, Iwata et al. 2009).

To realize the potential of stem cell therapy for periodontal regeneration, effective methods to extract and expand ''human'' PDL (hPDL) cells have to be established. Somerman et al. (1988) first reported on a method to culture PDL cells, and the method has been widely used because of its clear concept, ''Extract cells from the mid-third of teeth''. However, the proliferation of the cells was slow, and it took a great deal of time to expand the PDL cells required for transplantation. Therefore, recent studies have combined the use of enzymatic digestion and this concept to obtain a higher yield of cells (Seo et al. 2004, Sonoyama et al. 2006, Liu et al. 2008). Still, the characteristics of PDL cells remain to be elucidated, although some PDL-specific genes were proposed (Duarte 1998, Horiuchi et al. 1999, Yamada et al. 2001, Lallier et al. 2005, Nakamura et al. 2005, Nishida et al. 2007, Pi et al. 2007).

In this study, 41 teeth were collected from human patients, and the culture condition of hPDL cells was optimized. Moreover, distinguishable hPDL markers were confirmed for the identification of hPDL cells, and the potential of hPDL cells in tissue regeneration was evaluated both in vitro and in vivo.

Materials and Methods

This study was conducted according to the principles expressed in the Declaration of Helsinki. The study was approved by the Institutional Review Board of Tokyo Women's Medical University Human Subjects Research. All patients or guardians were fully informed and gave written consent for the donation of their teeth and their subsequent use in this research project.

All animal procedures were approved by the Institutional Animal Care and Use Committee of Tokyo Women's Medical University.

Cell culture

Normal human teeth were extracted for orthodontic or impaction reasons from 41 patients between 14 and 57 years of age at Tokyo Women's Medical University Hospital. The age, sex, and position of the extracted tooth from the donors are shown in Table 1. First, each tooth was rinsed five times with antibiotics (Unasyn) (Pfizer Japan, Tokyo, Japan). Then, the PDL tissue was gently separated from the surface of the mid-third of root and subsequently digested with trypsin/EDTA (0.25% trypsin and 1 mM EDTA) (Invitrogen, Carlsbad, CA, USA) or a solution of collagenase type I (varying concentrations) (SERVA Electrophoresis, Heidelberg, Germany) with 1200 PU/ml dispase (Godo Syusei, Tokyo, Japan) in α-MEM glutamax (Invitrogen) for 60 min. at 37°C with vigorous shaking. Single-cell suspensions were obtained by passing the cells through a 70 μm strainer (Falcon, Franklin Lakes, NJ, USA). After being strained, the

Table 1. Isolation and ALP activity of hPDL cells

#	Age (years)	Sex	Position	Enzyme	Cell expansion	ALP induction
1	19	F	18	T	+	+
2	41	M	28	T	+	+
3	34	F	38	T	+	–
4	34	F	28	T	+	–
5	14	M	22	T	+	+
6	14	M	34	T	–	
7	24	F	38	T	+	+
8	26	M	38	T	+	+
9	26	M	18	T	+	+
10	30	F	42	T	–	
11	24	F	24	C/D	+	+
12	24	F	14	C/D	+	+
13	26	F	38	T	–	
14	25	F	38	C/D	+	+
15	19	F	38	C/D	+	+
16	32	F	48	C/D	+	+
17	26	F	48	C/D	+	+
18	30	M	28	C/D	+	+
19	57	F	18	C/D	+	+
20	25	M	18	C/D	+	+
21	57	F	28	C/D	+	+
22	18	M	28	C/D	+	+
23	30	F	28	C/D	+	+
24	25	F	48	C/D	+	+
25	19	F	48	C/D	+	+
26	57	F	38	C/D	+	+
27	35	M	38	C/D	+	+
28	23	M	38	C/D	–	
29	47	M	48	C/D	+	+
30	31	M	48	C/D	+	+
31	57	F	28	C/D	+	+
32	23	F	38	C/D	+	+
33	45	M	48	C/D	+	+
34	32	M	48	C/D	+	+
35	25	M	48	C/D	+	+
36	30	F	38	C/D	+	+
37	31	F	38	C/D	+	+
38	34	F	48	C/D	+	+
39	27	F	38	C/D	+	+
40	30	F	48	C/D	+	+
41	25	M	28	C/D	+	+

hPDL tissues from 41 patients were digested with trypsin–EDTA (T) or collagenase/dispase (C/D) and cultured. Tooth position was indicated by means of Zsigmondy and Palmer system (Peck & Peck, 1993). Cell expansion was judged from the microscopic view on Day 7 after the spreading. Expanded cells at Passages 3–5 were cultured with or without osteoinductive supplements (50 μg/ml ascorbic acid, 10 mM β-glycerophosphate, and 10 nM dexamethasone), then ALP activity was measured and enhanced cells were considered as ALP induction positive (+).
ALP, alkaline phosphatase; hPDL, human periodontal ligament; F, female; M, male.

cells were plated onto a T25 Primaria™ culture flask (Falcon) (Passage 0). The cells were then cultured in complete culture medium [α-MEM glutamax containing 10% foetal bovine serum (FBS) (Moregate Biotech, Bulimba, Queensland, Australia), and 1% penicillin/streptomycin (Sigma-Aldrich, St Louis, MO, USA)]. After 48 h, unattached cells and debris were washed out, and new medium was added. The cells were subcultured using trypsin/EDTA on Day 5, and spread out on a T75 Primaria™ culture flask (Passage 1). Subculture was performed every 3–4 days until Passage 3. Thereafter, cells were plated at a density of 50 cells/cm^2 on 60 cm^2 culture dishes every 14 days until their proliferation potential was lost.

Human gingival fibroblasts (hGFs) from three different donors were purchased from ScienCell (Carlsbad, CA, USA). These hGFs were cryopreserved at Passage 1 and delivered frozen. Experiments were carried out with cells from the third to fifth passages. Three different lots of human bone marrow-derived mesenchymal stem cells (hBMMSCs) and human adipose-derived stem cells (hADSCs) were purchased from Cellular Engineering Technologies (Coralville, IA, USA). Similarly and unless otherwise noted, experiments were carried out with cells from the third to fifth passages. All cells were cultured in complete culture medium as described above.

Colony-forming assay

The cells were plated at a density of 100 cells/60 cm^2 dish, and cultured in complete medium for 14 days. The cells were stained with 0.5% crystal violet in methanol for 5 min. as previously described (Nimura et al. 2008). The cells were washed twice with distilled water, and the number of colonies was counted. Colonies <2 mm in diameter and/or faintly stained were ignored.

Alkaline phosphatase (ALP) activity

The cells were plated on 96-well plates at a density of 1×10^4 cells/well and cultured in complete medium for 48 h. Then, the medium was changed to complete medium with or without various concentrations of osteoinductive supplements, ascorbic acid (AA) (Wako Pure Chemical, Tokyo, Japan), β-glycerophosphate (βGP) (Sigma-Aldrich), and/or dexamethasone (DEX) (Fuji Pharma, Tokyo, Japan). After five additional days of culture, the cells were washed once with normal saline solution, and ALP activity was evaluated after incubation with 10 mM *p*-nitrophenylphosphate as a substrate in 100 mM 2-amino-2-methyl-1, 3-propanediol–HCl buffer (pH 10.0) containing 5 mM $MgCl_2$ for 5 min. at 37°C. The addition of NaOH quenched the reaction, and the absorbance at 405 nm was measured using a plate reader (Bio-Rad Model 450, Bio-Rad, Hercules, CA, USA).

Differentiation assay

For osteogenesis studies, 50 cells were plated in 60 cm^2 dishes and cultured for 14 days as described previously (Nimura et al. 2008) with slight modifications. The medium was then switched to a calcification medium consisting of complete medium supplemented with 50 μg/ml AA, 10 mM βGP, and 10 nM DEX (osteoinductive medium) for an additional 21 days. These dishes were stained with 1% alizarin red solution, and alizarin red-positive colonies were counted. The same calcification cultures were subsequently stained with crystal violet, and the total cell colonies were counted. Colonies that were <2 mm in diameter or appeared yellowish were ignored.

For adipogenesis experiments, 50 cells were plated in 60 cm^2 dishes and cultured in complete medium for 14 days. The medium was then switched to adipogenic medium, which consisted of complete medium supplemented with 100 nM DEX, 0.5 mM isobutyl-1-methyl xanthine (Sigma-Aldrich), and 50 μM indomethacin (Wako Pure Chemical) for an additional 21 days. The adipogenic cultures were fixed with 4% paraformaldehyde and stained with fresh oil red O solution, and the numbers of the oil red O-positive colonies were counted. Colonies that were <2 mm in diameter or ones that appeared faint were ignored. The cultures were then stained with crystal violet, and the total number of cell colonies was counted.

For chondrogenesis studies, 250,000 cells were placed in a 15 ml polypropylene tube (Becton Dickinson, Mountain View, CA, USA) and centrifuged for 10 min. The pellet was cultured in chondrogenesis medium [high-glucose Dulbecco's modified Eagle's medium (Invitrogen) supplemented with 500 ng/ml bone morphogenetic protein 2 (R&D Systems, Minneapolis, MN, USA), 10 ng/ml transforming growth factor β3 (R&D Systems), 10 nM DEX, 50 μg/ml AA, 40 μg/ml proline, 100 μg/ml pyruvate, and 50 mg/ml ITS+Premix (Becton Dickinson)]. The medium was replaced every 3–4 days for 21 days.

For immunohistochemical staining, the pellets were embedded in OCT compound, and the specimen block was cut into 5 μm frozen tissue sections. After being dried for 1 h at room temperature, the tissue sections were treated with chondroitinase ABC (0.25 U/ml) (Seikagaku Biobusiness, Tokyo, Japan) and hyaluronidase (type I-S) (Sigma-Aldrich) for 30 min. at 37°C. The sections were washed with Tris-buffered saline (TBS) (Takara Bio, Shiga, Japan), and incubated with TBS containing 5% donkey serum and 0.3% Triton X for 1 h to block non-specific reactions. The sections were then incubated with a mouse monoclonal antibody against human type II collagen (1:100 dilution) (Daiichi Fine Chemical, Toyama, Japan) for 12 h at 4°C. The slides were again washed three times with TBS and incubated with a horseradish peroxidase-conjugated secondary antibody (1:1000 dilution) (Jackson ImmunoResearch Laboratories, West Grove, PA, USA) for 1 h at room temperature. Immunostaining was detected by 3, 3′-diaminobenzidine (DAB), and the counterstaining was performed with Mayer's haematoxylin.

Isolation of RNA and polymerase chain reaction (PCR)

Total RNA was isolated with a QIA shredder and RNeasy Mini kit (Qiagen, Valencia, CA, USA) according to the manufacturer's instructions. Thereafter, cDNA was synthesized from 500 ng of the total RNA using the Superscript VILO cDNA Synthesis Kit (Invitrogen). β-Actin was utilized as the internal control gene from the results observed on the TaqMan Human Endogenous Control Plate (Applied Biosystems, Foster City, CA, USA). The mRNA expression levels of periodontal marker genes and osteogenic genes were quantitatively analysed by real-time PCR (ABI Prism 7300 Sequence detection system, Applied Biosystems) using sequence-specific primers. The primers used were as follows: asporin (Hs00214395_m1), β-actin (4326315E), bone sialoprotein (BSP; Hs00173720_m1), cementum protein 1 (CEMP1; Hs03004478_s1), cyclin J (Hs00908190_g1), FDC-SP (Hs00395131_m1), milk fat globule-EGF factor 8 protein (MFGE8; Hs00170712_m1), MSX1 (Hs00427183_m1), MSX2 (Hs00741177_m1), neural cell adhesion molecule 1 (NCAM1;

Hs00941821_m1), osteocalcin (OCN; Hs01587813_g1), osteopontin (OPN; Hs00167093_m1), periostin (Hs00170815_m1), S100A4 (Hs00243202_m1), and type II collagen (Col2A1; Hs01060345_m1). The samples were analysed in triplicate. The mRNA expression levels relative to β-actin were determined, and, in some cases, the fold changes were calculated using the values obtained by means of the $2^{-\Delta\Delta C_t}$ method at each time point (Livak & Schmittgen 2001).

PCR array

Human osteogenesis RT^2 Profiler™ PCR Array and Human Cell Surface Markers RT^2 Profiler™ PCR Array (SuperArray Bioscience, Bethesda, MD, USA) were used to screen for the expression of multiple genes in hPDL cells, hBMMSCs, and hGFs according to the manufacturer's protocol, and the levels of gene expression were determined with the comparative C_t method.

Flow cytometric assay

One million cells were suspended in 100 μl Dulbecco's phosphate-buffered saline (PBS) containing 10 μg/ml of each specific antibody. For determining the surface markers, fluorescein isothiocyanate (FITC)- or phycoerythrin (PE)-coupled antibodies against CD29, CD34, CD44, CD90, CD106, and CD146 (Becton Dickinson), ALP (R&D systems), STRO-1 (Santa Cruz Biotechnology, Santa Cruz, CA, USA), CD14 and CD45 (Biolegend, San Diego, CA, USA), and CD105 (Ancell, Bayport, MN, USA) were used. As the isotype control, FITC- or PE-coupled non-specific mouse IgG (Becton Dickinson), and PE-coupled non-specific mouse IgM (Antigenix America, Huntington Station, NY, USA) were substituted for the primary antibodies. After being incubated for 30 min. at 4°C, the cells were washed with PBS and then suspended in 1 ml of PBS for further analysis. Cell fluorescence was determined using a flow cytometer (Epics-XL; Beckman Coulter, Fullerton, CA, USA).

Immunohistochemistry

A human tooth surrounded by alveolar bone was subjected to immunohistochemistry. The tissue was fixed with 4% paraformaldehyde and decalcified with neutralized 10% EDTA (pH 7.4) at 4°C for 2 weeks before dehydration and paraffin embedding. Sections that were 5 μm thick were collected on glass slides. To enhance antigen retrieval, the slides were immersed in 1% antigen unmasking solution (Vector Laboratories, Burlingame, CA, USA) and blocked for 30 min. at room temperature with non-immune rabbit serum, followed by a 16-h incubation with the specific primary antibodies. The primary antibodies and dilutions used were anti-human S100A4 (1:100) (ab27957; Abcam, Cambridge, UK) and anti-human periostin (1:100) (ab14041; Abcam). The slides were then rinsed, followed by incubation for 30 min. at room temperature with biotinylated secondary antibody (1:200) (Vectastain ABC kit AK-5002; Vector Laboratories). The slides were washed with PBS, and the avidin–biotin complex was added for 30 min. at room temperature. The slides were then rinsed well with PBS and developed with DAB.

Transplantation

hPDL cells at Passage 5 were seeded on temperature-responsive culture dishes (35 mm in diameter, UpCell®, CellSeed, Tokyo, Japan) at a cell density of 3×10^4 cells/dish and cultured in complete medium for 2 days. Then, the culture medium was changed to an osteoinductive medium, and the cells were cultured for an additional 14 days. For harvesting cell sheets, the temperature was reduced to room temperature. Then, the culture medium was aspirated, and a wet sheet of woven polyglycolic acid (PGA) (Neoveil®, PGA Felt-Sheet Type, 0.15 mm in thickness; Gunze, Tokyo, Japan) was used for multi-layering, as described previously (Iwata et al. 2009). Because the PGA sheets stuck to the cell sheets within several seconds, PGA sheets holding cell sheets were harvested by peeling them from the dishes with forceps. This procedure was repeated, and eventually four, six, eight, and 10 layers of hPDL cell sheets were obtained. F344 athymic rats (6-week-old male; Charles River Japan, Tokyo, Japan) were anaesthetized with 2% inhaled isoflurane and ventilated using a rodent mechanical ventilator. Incisions were made subcutaneously on the dorsa of the rats. Multilayered hPDL cell sheets–PGA constructs were placed at the muscle surfaces, and the incisions were closed with 5-0 silk sutures (Nesco-suture; Alfresa, Osaka, Japan). After 3 days, 10 days, or 4 weeks, the transplanted grafts were resected for histological analysis. Three animals were used for each time point. The specimens were fixed with 4% paraformaldehyde and routinely processed into 7-μm-thick paraffin-embedded sections. The paraffin sections were stained with either haematoxylin–eosin or alizarin red.

Data analysis

All values are expressed as means ± SD. All samples were analysed by Student's t-tests. Values of $p < 0.05$ were considered statistically significant.

Results

Extraction and characterization of hPDL cells

A total of 41 teeth (36 wisdom teeth and five other teeth) (Table 1) were obtained and digested with either collagenase/dispase or trypsin/EDTA, both of which were conventionally used for tissue dissociation. The success rate of cell expansion with collagenase/dispase [29/30 (96.7%)] was higher than with trypsin/EDTA [8/11 (72.7%)]. In some trypsin/EDTA-digested samples, no ALP induction of hPDL cells was observed (2/8). Because of the small quantity of hPDL tissue, the initial cell density was extremely low (usually < 50 cells/cm^2) even when the small culture flask (T25) was used. hPDL cells proliferated clonally, and the population doubling time was < 24 h for 50 days (Fig. 1a). The colony-forming efficiency of hPDL cells was approximately 30% at Passage 1 and increased with every passage (Fig. 1b). The proliferation rates of hPDL cells were higher when they were spread at lower densities (Fig. 1c). AA, βGP, or DEX treatment enhanced the ALP activity of hPDL cells in a dose-dependent manner, and their use in combination maximized the increase in ALP activity (Fig. 1d). In contrast, no induction of ALP activity was observed in hGFs (data not shown).

The osteogenic, adipogenic, and chondrogenic potentials of hPDL cells were investigated in comparison with that of hADSCs, hBMMSCs, and hGFs. Similar to hADSCs and hBMMSCs, hPDL cells showed high osteogenic potential (~60% of total colonies) (Fig. 2a and b). In contrast, no alizarin red-positive colony was observed in hGFs. In the adipogenic studies, hADSCs and hBMMSCs showed significant potential (~ 85%) compared

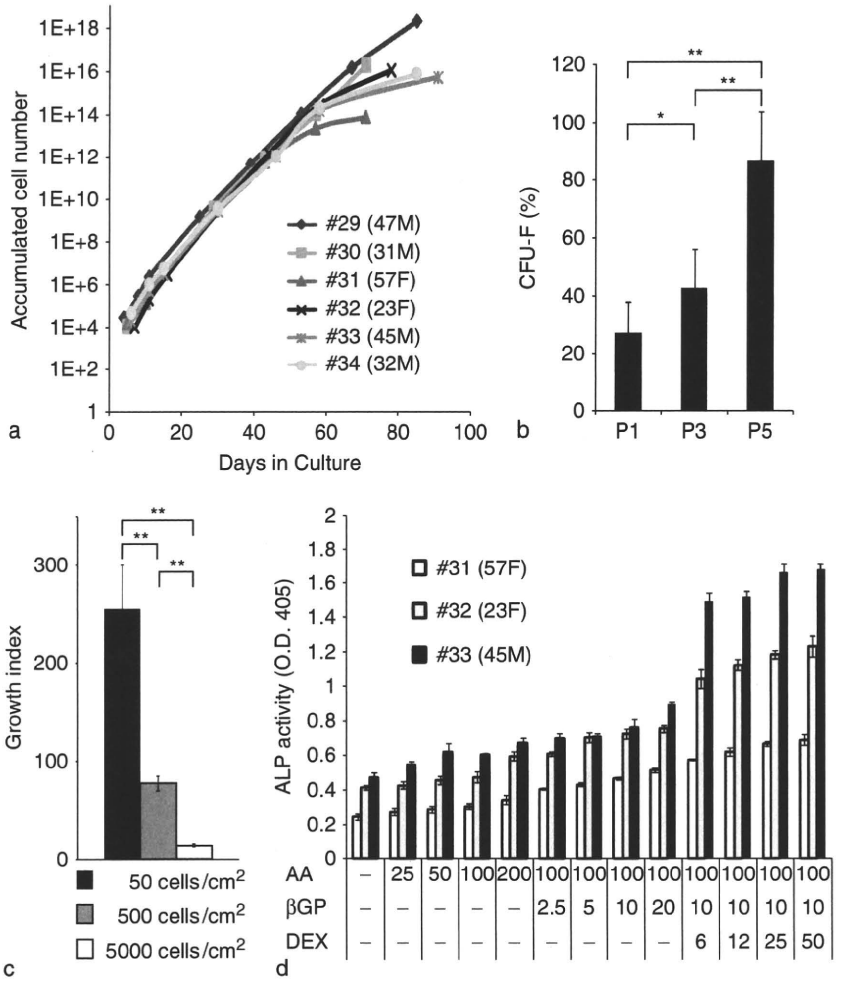

Fig. 1. Proliferation, colony-forming unit-fibroblast (CFU-F), and alkaline phosphatase (ALP) activity of human periodontal ligament (hPDL) cells. (a) The growth and proliferative life span of hPDL cells from six different donors. Cells were seeded and subcultured at 50 cells/cm^2 every 2 weeks after Passage 3. (b) CFU-F of hPDL cells. hPDL cells from six donors were examined for colony-forming assay at Passages 1, 3, and 5 in triplicate. The bars and lines represent the means and SD of six samples. Statistically significant difference ($^*p<0.05$; $^{**}p<0.01$). (c) Effect of the seeding density on the proliferation of hPDL cells. Cells were plated in triplicate at densities of 50, 500, and 5000 cells/cm^2, respectively. Medium was changed 24 h after seeding, and hPDL cells were cultured for an additional 7 days. The bars and lines represent the means and SD of three samples at Passage 3. **Statistically significant difference ($p<0.01$). (d) ALP activity of hPDL cells from three donors induced by the use of a combination of osteoinductive reagents, ascorbic acid (AA) (μg/ml), β-glycerophosphate (βGP) (mM), and dexamethasone (DEX) (nM). The bars and lines represent the means and SD.

with that of hPDL cells and hGFs (~30%) (Fig. 2c and d). In the chondrogenic studies, hPDL cells differentiated into chondrocytes, which were positive for type II collagen antibody (Fig. 2e). Real-time PCR analyses showed that type II collagen expression was detectable in all types of cells (Fig. 2f) and hBMMSCs had a higher expression of type II collagen than other cells. hGFs appeared to have a higher expression of type II collagen than hPDL cells. However, there was no significant difference in type II collagen expression among hPDL cells, hADSCs, and hGFs.

Next, we investigated the time course expression of osteogenic genes, OCN, OPN, and BSP, in hPDL cells. When hPDL cells were cultured in complete medium supplemented with AA, βGP, and DEX, the expression levels of OCN, OPN, and BSP were maximized on Day 14 (Fig. 3a), and an alizarin red-positive area was clearly observed at the same time (Fig. 3b). However, the expression levels of all three genes were decreased on Day 21. When hPDL cells were cultured with AA and βGP, but without DEX, the gene expression levels of OCN, OPN, and BSP were increased up to Day 21.

Surface epitopes of hPDL cells

The expression of putative mesenchymal stem cell markers (CD29, CD44, CD90, and CD105 positive, and CD14, CD34, and CD45 negative) was observed in all types of cells (Fig. 4). CD146, CD106, and ALP were more frequently positive in hPDL cells compared with hGFs. STRO-1, an epitope originally suggested as a marker for MSCs, was expressed in <20% of cells for all types of cells.

Gene expression profile

Previous studies demonstrated that hPDL cells have osteogenic potential. Thus, we performed both osteogenesis and cell surface markers PCR array on hPDL cells and compared it with hBMMSCs (Table 2A) or hGFs (Table 2B). Several genes were preferentially expressed in hPDL cells. Neural cell adhesion molecule 1 (NCAM1) was strongly expressed in hPDL cells compared with hBMMSCs and hGFs. This difference was statistically significant. In addition to these PCR arrays, each of the known PDL marker genes was also verified with a TaqMan® gene expression assay. β-Actin was chosen as the endogenous control from the results of the TaqMan® Human Endogenous Control Plate because of the stability of the signal between the cell types and its level of expression (data not shown). The expression levels of MSX1, NCAM1, and S100A4 in hPDL cells were higher than in hBMMSCs (Fig. 5a). Moreover, the expression levels of NCAM1 and periostin in hPDL cells were higher than in hGFs (Fig. 5a). The immunohistochemical analyses confirmed the positive signals of both S100A4 and periostin in hPDL tissues between the alveolar bone and dentin (Fig. 5b–e).

Transplantation

To verify the osteogenic potential in vivo, multi-layered hPDL cell sheets were transplanted into the backs of athymic rats. After being cultured with an osteoinductive medium for 14 days, hPDL cells were multi-layered (four,

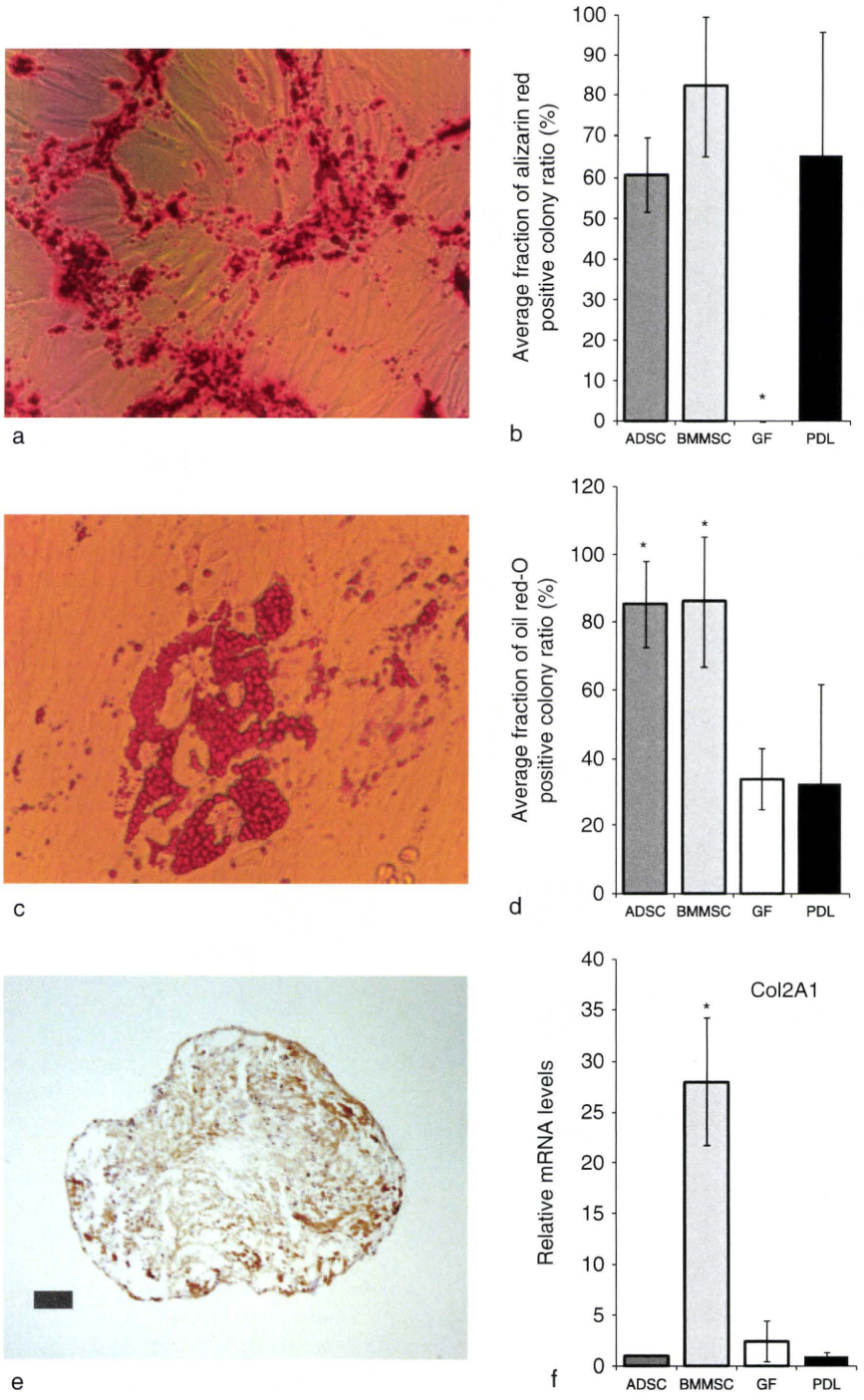

Fig. 2. Differentiation potential of human periodontal ligament (hPDL) cells. (a) hPDL cells positively stained with alizarin red. hPDL cells were cultured for 21 days in osteoinductive medium. (b) The ratio of alizarin red-positive colonies in the total number of colonies. Each sample was examined in triplicate, and the means of each sample were used for statistical analysis. The bars and lines represent the means and SD of human adipose-derived stem cells (hADSCs) ($n = 3$), human bone marrow-derived mesenchymal stem cells (hBMMSCs) ($n = 3$), human gingival fibroblasts (hGFs) ($n = 3$), and hPDL cells ($n = 7$). $^*p < 0.05$ *versus* hPDL cells. (c) hPDL cells positively stained with oil red O. hPDL cells were cultured for 21 days in adipogenic medium. (d) The ratio of oil red O-positive colonies in the total number of colonies. Each sample was examined in triplicate, and the means of each sample were used for statistical analysis. The bars and lines represent the means and SD of hADSCs ($n = 3$), hBMMSCs ($n = 3$), hGFs ($n = 3$), and hPDL cells ($n = 7$). $^*p < 0.05$ *versus* hPDL cells. (e) Immunohistochemical analysis for type II collagen. hPDL cells were pelleted and cultured for 21 days in the defined medium described in the ''Materials and Methods''. A macro picture of cartilage pellets with 100 μm scale is shown. (f) Gene expression analysis for type II collagen on Day 21 was analysed by real-time PCR. The bars and lines represent the means and SD of hADSCs ($n = 3$), hBMMSCs ($n = 3$), hGFs ($n = 3$), and hPDL cells ($n = 7$). The mean fold changes in gene expression relative to β-actin were calculated using the values obtained from hPDL cells as a calibrator by means of the $2^{-\Delta\Delta C_t}$ method (Livak & Schmittgen 2001). $^*p < 0.05$ *versus* hPDL cells.

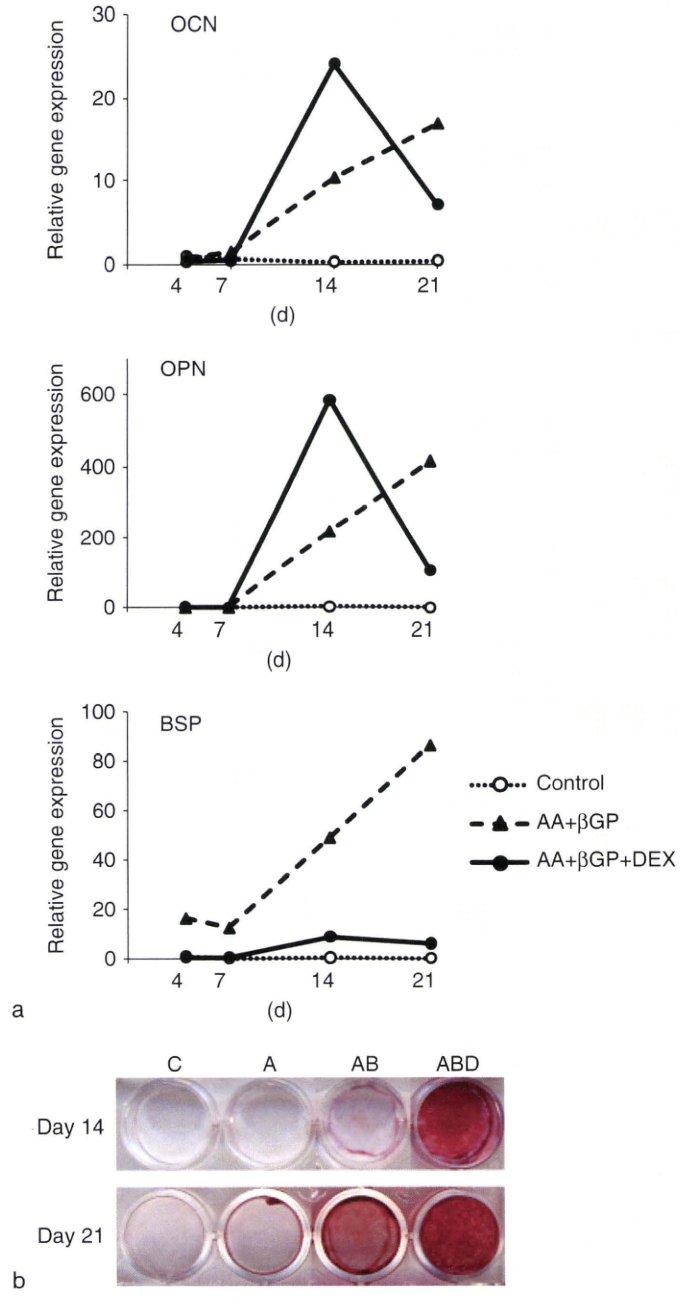

Fig. 3. Osteoblastic/cementoblastic gene expression during osteoinduction in human periodontal ligament (hPDL) cells. (a) Effects of osteoinductive supplements on the expression of osteocalcin (OCN), osteopontin (OPN), and bone sialoprotein (BSP). After hPDL cells were treated with or without supplements [AA (50 μg/ml)+βGP (10 mM) or AA+βGP+DEX (10 nM)], the gene expression at various time points (4–21 days) was analysed by real-time PCR. Two individual PDL cells were examined in triplicate, and the average values are shown. The mean fold changes in gene expression relative to β-actin were calculated using the values obtained from hPDL cells without induction on Day 4. (b) Alizarin red staining of hPDL cells cultured with or without osteoinductive supplements. PDL cells were spread at a density of 5000 cells/cm^2. After 48 h, the culture medium was switched to complete medium only (c) or complete medium+AA (50 μg/ml) (A); AA+βGP (10 mM) (AB); or AA+βGP+DEX (10 nM) (ABD), and cultured for 14 or 21 days.

six, eight, or 10 layers) with woven PGA and transplanted into the backs of athymic rats. Layering structures were clearly seen on Day 3 (Fig. 6a and b). An area that was alizarin red positive was observed on Day 3, and it grew until Day 10 in both eight- and 10-layer transplantation.

Discussion

Human teeth are routinely extracted because of caries or orthodontic reasons, even though they retain healthy PDL or pulp tissues. Therefore, researchers have utilized dental stem cells as non-invasive cell sources for regenerative medicine. In fact, PDL cells (Nakahara et al. 2004, Sonoyama et al. 2006, Liu et al. 2008, Iwata et al. 2009) and dental pulp cells (Iohara et al. 2004, 2006) have already been examined for their regenerative potential in large animal models. Importantly, the clinical outcomes of these studies were superior to those of traditional therapies. Thus, human clinical trials using hPDL cells have the potential to treat various defects, which have until now been thought to be difficult to cure. Although the prospects are increasing, appropriate methods for extracting and expanding hPDL cells are still not well established. In this study, we determined the optimal method for the isolation and expansion of hPDL cells. We then examined their gene expressions and differentiation potentials and eventually validated the common characteristics of hPDL cells from 41 samples.

First, the method of enzymatic digestion for hPDL tissues was optimized. Because hPDL tissue mainly consists of collagen, the dose–response effect of collagenase (0.075, 0.75, and 1.5 PZ-U/ml) was studied, resulting in 0.75 PZ-U/ml as the optimal concentration (data not shown). The success rate of cell expansion with collagenase/dispase was 96.7% (29/30), which was superior to the original explant method (76%) (Somerman et al. 1988). Only one sample (#28, a 23-year-old male) exhibited bacterial contamination during the initial days of culture. Trypsin/EDTA also extracted cells from hPDL tissues (72.7%). However, some of the samples lost their osteogenic potential (Table 1) and had low proliferation (data not shown). Thus, collagenase/dispase was chosen for further studies. Primaria culture dishes were used in this study because the initial cell attachment was enhanced compared with normal Falcon dishes (data not shown). The cells were cultured in α-MEM glutamax for rapid cell expansion as described previously (Sotiropoulou et al. 2006). hPDL cells exhibited an increased proliferation compared with other mesenchymal tissue-derived cells (Matsubara et al. 2005, Sakaguchi et al. 2005). Usually, the number of hPDL

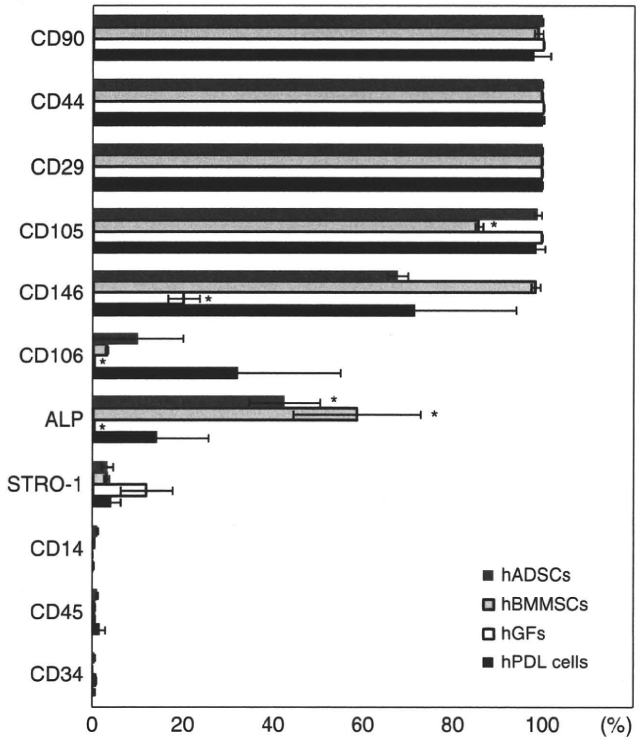

Fig. 4. Surface molecule characterization by flow cytometry. Expression of cell surface proteins on human adipose-derived stem cells (hADSCs), human bone marrow-derived mesenchymal stem cells (hBMMSCs), human gingival fibroblasts (hGFs), and human periodontal ligament (hPDL) cells as determined by flow cytometry. The bars and lines represent the means and SD of three samples from each source. $^{*}p<0.05$ *versus* hPDL cells.

Table 2A. Differentially expressed genes between hPDL cells and hBMMSCs by PCR array

Name of gene	Description	Fold up- or down-regulation	*p*-value
NCAM1	Neural cell adhesion molecule 1	27.10	0.0001
MSX1	Msh homeobox 1	15.55	0.0011
FLT1	Fms-related tyrosine kinase 1 (vascular endothelial growth factor)	12.74	0.0287
BMP4	Bone morphogenetic protein 4	6.14	0.0213
HLA-DRA	Major histocompatibility complex, Class II, DRα	5.95	0.2112
IL12RB1	Interleukin 12 receptor, β1	5.83	0.0060
CD40	CD40 molecule, TNF receptor superfamily member 5	5.64	0.0189
COL14A1	Collagen, type XIV, α1	4.41	0.3085
CD24	CD24 molecule	−4.05	0.1410
CD36	CD36 molecule (thrombospondin receptor)	−4.23	0.1536
CD70	CD70 molecule	−4.57	0.2035
ST6GAL1	ST6 β-galactosamide α-2,6-sialyltranferase 1	−4.81	0.0012
BMP6	Bone morphogenetic protein 6	−5.30	0.0050
ITGA2	Integrin, α2 (CD49B, α2 subunit of VLA-2 receptor)	−6.27	0.0510
KRT18	Keratin 18	−9.06	0.0102
KRT8	Keratin 8	−9.74	0.0044
DPP4	Dipeptidyl-peptidase 4 (CD26, adenosine deaminase complexing protein 2)	−14.06	0.0579
COMP	Cartilage oligomeric matrix protein	−56.27	0.0024
TEK	TEK tyrosine kinase, endothelial (venous malformations, multiple cutaneous and	−109.90	0.0001

Three different individuals of hPDL cells and hBMMSCs were examined with "cell surface markers" and "osteogenesis" PCR arrays and statistical analyses were performed. Genes with defined threshold of 4-fold differential expression are listed. If hPDL cells >hBMMSCs, "+"; if hPDL cells <hBMMSCs, "−". A grey box indicates a statistically significant change. $P<0.05$. hPDL, human periodontal ligament; hBMMSCs, bone marrow-derived mesenchymal stem cells.

cells exceeded 1 million within the first 2 weeks. hPDL cells become senescent after 70–100 days of cultivation, and no transformation of cells was observed in this study. The colony-forming efficiency of hPDL cells was in agreement with previous studies (Nagatomo et al. 2006). Surprisingly, the colony-forming efficiency of hPDL cells increased with every passage. Therefore, it is possible that the method of cell expansion used in this study, in which seeding density was low, exclusively selected highly proliferative and replicative hPDL cells.

Next, the gene expression of hPDL cells was examined. Generally speaking, hPDL cells have higher ALP activity than that of hGFs and possess osteogenic potential (Somerman et al. 1988, Murakami et al. 2003). All hPDL samples extracted with collagenase/dispase exhibited such characteristics, suggesting that the experiment was properly conducted. The effect of osteoinductive supplements, AA, βGP, and DEX, on ALP activity of hPDL cells was investigated, and the maximum induction was determined to be as much as the conventional concentration of an osteoinductive medium (50 μg/ml AA, 10 mM βGP, and 10 nM DEX).

In differentiation assays, the method described by Sekiya et al. (2002) was used because this method could simultaneously evaluate the rate of differentiation potentials as well as the colony-forming efficiency. hPDL cells differentiated into the osteoblastic lineage with high frequency as much as that of hADSCs and hBMMSCs. Furthermore, the expression of osteoblastic genes during osteoinduction was also investigated to determine the optimal culture period for hPDL cells. When DEX was used in addition to AA and βGP, the expression levels of OCN, OPN, and BSP were maximized on Day 14 and were decreased on Day 21. It is known that the continuous presence of DEX can modulate differentially the osteoblastic phenotypes of cells (Hoemann et al. 2009). Considering the culture condition of this study, in which AA, βGP, and DEX were continuously supplied, it was quite presumable that the expression of these genes was modified by the long-term DEX treatment. Similar results were observed by Zhou et al. (2008) using hPDL cells. Alizarin red staining also confirmed that cultivation for 14 days was enough to form mineralized nodules when cells were cultured with AA, βGP, and

Table 2B. Differentially expressed genes between hPDL cells and hGFs by PCR array

Name of gene	Description	Fold up- or down-regulation	*p*-value
HLA-DRA	Major histocompatibility complex, Class II, DRα	30.30	0.0557
VCAM1	Vascular cell adhesion molecule 1	23.88	0.0269
ALPL	Alkaline phosphatase, liver/bone/kidney	23.25	0.0486
TPSAB1	Tryptase α/β1	20.98	0.0216
NCAM1	Neural cell adhesion molecule 1	19.53	0.0456
COL14A1	Collagen, type XIV, α1	9.46	0.1882
FGFR2	Fibroblast growth factor receptor 2	7.04	0.0019
TGFB3	Transforming growth factor β3	6.77	0.0310
MYOCD	Myocardin	6.22	0.3872
CD4	CD4 molecule	5.79	0.3811
ITGAM	Integrin, αM (complement component 3 receptor 3 subunit)	5.39	0.0178
CD74	CD74 molecule, major histocompatibility complex, Class II invariant	5.34	0.3486
BGN	Biglycan	4.75	0.0652
EGF	Epidermal growth factor (β-urogastrone)	4.25	0.0658
IGF1	Insulin-like growth factor 1 (somatomedin C)	4.20	0.2378
ITGA2	Integrin, α2 (CD49B, α2 subunit of VLA-2 receptor)	−5.10	0.0830
COL15A1	Collagen, type XV, α1	−6.38	0.3418
CTSK	Cathepsin K	−7.22	0.0301

Three different individuals of hPDL cells and hGFs were examined with ''cell surface markers'' and ''osteogenesis'' PCR arrays and statistical analyses were performed. Genes with defined threshold of four-fold differential expression are listed. If hPDL cells >hGFs, ''+''; if hPDL cells <hGFs, ''−''. A grey box indicates a statistically significant change. $p<0.05$.
hPDL, human periodontal ligament; hGFs, human gingival fibroblasts.

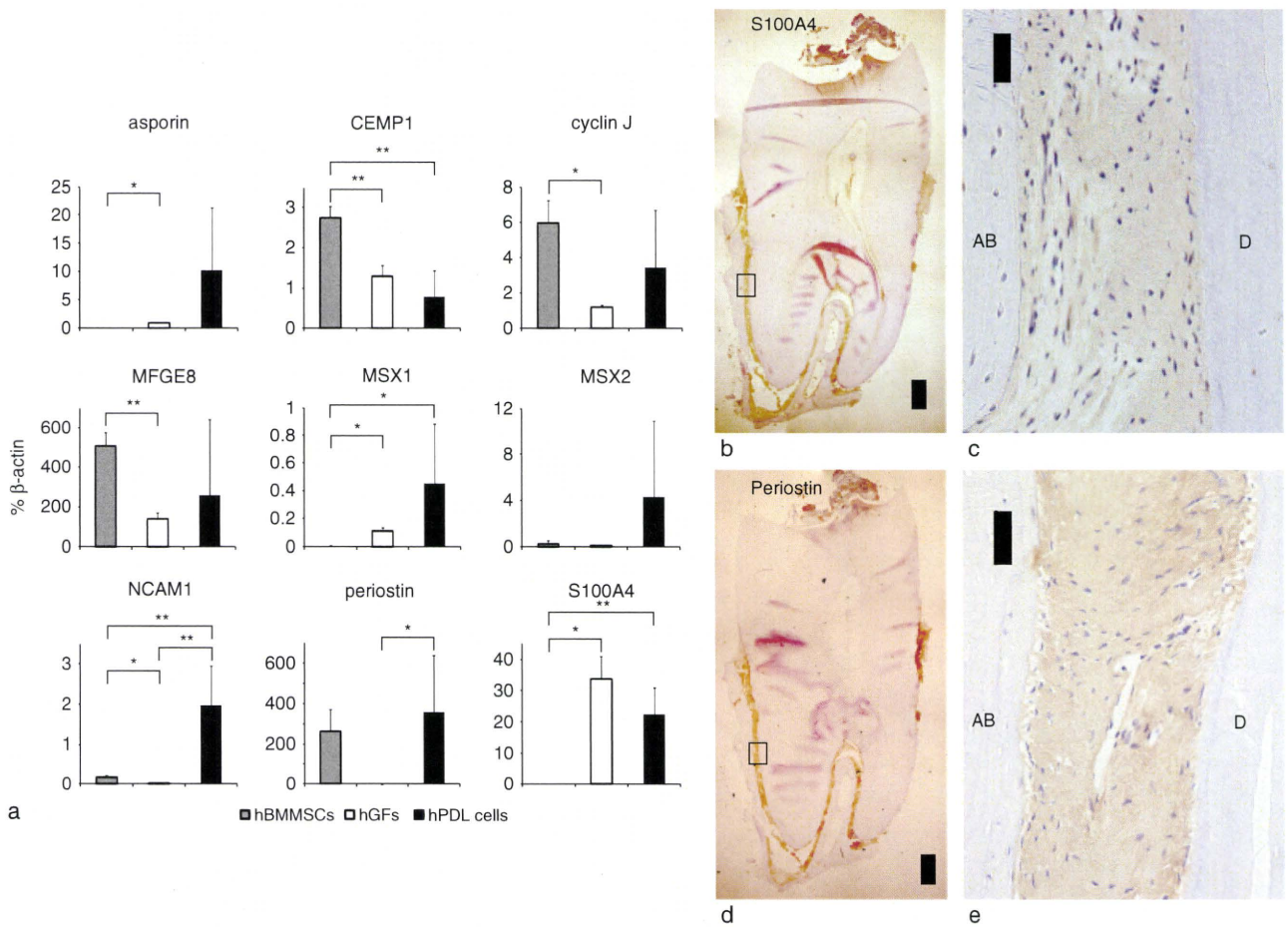

Fig. 5. Expression of PDL-specific markers. (a) Real-time PCR analysis of known PDL-specific genes. The bars and lines represent the means and SD of human bone marrow-derived mesenchymal stem cells (hBMMSCs) ($n = 3$), human gingival fibroblasts (hGFs) ($n = 3$), and human periodontal ligament (hPDL) cells ($n = 7$). Statistically significant difference ($^{*}p<0.05$; $^{**}p<0.01$). The tissue sections of a human tooth with surrounding bone were immunostained with anti-human S100A4 (b and c) or periostin (d and e) polyclonal antibodies. The positive staining is shown by a reddish-brown colour. All sections were counterstained with haematoxylin (blue). The scale bars, 1 mm (B and D) and 50 μm (C and E). AB, alveolar bone and D, dentin.

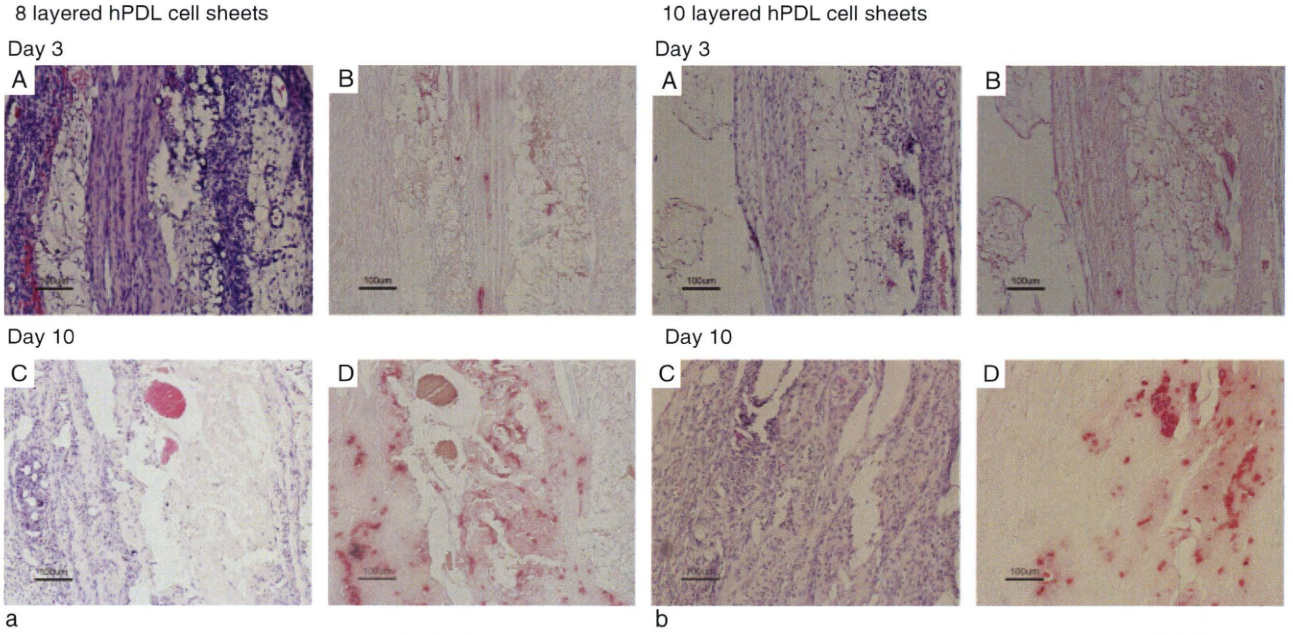

Fig. 6. The in vivo potential of multi-layered human periodontal ligament (hPDL) cell sheets that were subcutaneously transplanted in athymic rats. Eight (a)- or 10 (b)-layered hPDL cell sheets with woven PGA carrier were transplanted, and sacrificed on Day 3 (a and b) or Day 10 (c and d). The dissected samples were stained with haematoxylin–eosin (a and c) or alizarin red (b and d). The bars show 100 μm. Note that obvious alizarin red-positive areas are observed on Day 10 in both eight (a)- and 10 (b)-layered transplantation of hPDL cell sheets.

DEX. Thus, we concluded that osteoinductive cultivation with DEX for 14 days was sufficient to enhance the osteoblastic differentiation of hPDL cells.

Next, the adipogenic and chondrogenic potentials of hPDL cells were examined. Both potentials were lower in hPDL cells than in hADSCs or hBMMSCs. These results correlated with a previous report examining alveolar bone marrow-derived cells (Matsubara et al. 2005). It is possible that the origin of the cells may affect their potential. Both PDL tissue and alveolar bone are neural crest-derived mesenchymal stromal cells (Chai et al. 2000, Cho & Garant 2000). A recent study showed that neural crest-derived osteoblasts exhibited stronger bone formation activity than cells derived from the mesoderm (Leucht et al. 2008). Thus, further investigation is needed to clarify the origin-specific plasticity of hPDL cells.

In the adipogenic differentiation study, hGFs differentiated into oil red O-positive cells. It is possible that the method used in this study, where all cells have colony-forming ability, may affect the potential of adipogenic differentiation in hGFs. Additional studies should be undertaken to determine the differentiation properties of hGFs.

FCM analysis showed the similarity of surface epitopes among four types of cells. Putative markers for MSC (CD29, CD44, CD90, and CD90) were expressed in all kinds of cells. The expression of CD146, CD106, and ALP in hPDL cells was significantly higher than in hGFs, and these results agreed with those of other studies (Seo et al. 2004, Gronthos et al. 2006, Lindroos et al. 2008, Wada et al. 2009). In this study, only a small fraction of hPDL cells was STRO-1 positive ($4.2 \pm 2.0\%$). It is possible that the STRO-1 expression may be lost over time, as suggested in other studies (Matsubara et al. 2005, Zhou et al. 2008, Itaya et al. 2009).

Next, we studied the distinguishable marker genes of hPDL cells. Although similar approaches have been performed by others (Han & Amar 2002, Lallier et al. 2005, Fujita et al. 2007), the results of our PCR array showed NCAM1 as a new marker of hPDL cells. In addition, the proposed PDL markers (asporin, CEMP1, cyclin J, FDC-SP, MFGE8, MSX1, MSX2, periostin, and S100A4) (Ishikawa et al. 2009) were also investigated using commercially available PCR primer sets. The strong expression of both S100A4 and periostin was detectable in all hPDL cells. However, individual variability in the expression levels of asporin, MSX1, and MSX2 was observed. In this study, the expression of FDC-SP was rarely observed in all types of cells (data not shown), and no preferential expression of CEMP1, cyclin J, or MFGE8 was observed in hPDL cells (Fig. 5). It is possible that the culture conditions used in this study may affect the expression of these genes. Still, immunohistochemical studies confirmed that both S100A4 and periostin had specific signals in hPDL specimens. Thus, these two genes can be useful to identify hPDL cells.

To assess the in vivo osteogenic potential, multi-layered hPDL cell sheets cultured with osteoinductive medium were transplanted into athymic rats. Because no alizarin red-positive area was observed in the control sites, the calcification was speculated to be induced by transplanted hPDL cell sheets. The alizarin red-positive area was expanded dramatically on Day 10 compared with Day 3, suggesting that hPDL cells promoted calcium deposition around them. Unfortunately, we could observe no calcified tissues in 4-week samples. It is possible that immunorejection may occur in this subcutaneous transplantation model with athymic rats.

From these results, hPDL cells were successfully extracted, expanded, and examined, and the characteristics and distinguishable markers of hPDL cells were proposed. Because true periodontal regeneration was already reported in a canine model using similar methods (Iwata et al. 2009), the methods described in this study might be helpful

for the cultivation and validation of hPDL cells for human clinical application.

Acknowledgements

We thank Professor Emeritus Hideki Ogiuchi for his kind supports, Ichiro Sekiya for excellent technical support, Hiroaki Sugiyama for expert help with histology, and Machiko Miyoshi for kind support. The authors are grateful to Norio Ueno (Tokyo Women's Medical University) for his valuable comments and suggestions.

References

Andreasen, J. O. & Kristerson, L. (1981) The effect of limited drying or removal of the periodontal ligament. Periodontal healing after replantation of mature permanent incisors in monkeys. *Acta Odontologica Scandinavica* **39**, 1–13.

Bianco, P. & Robey, P. G. (2001) Stem cells in tissue engineering. *Nature* **414**, 118–121.

Chai, Y., Jiang, X., Ito, Y., Bringas, P. Jr., Han, J., Rowitch, D. H., Soriano, P., McMahon, A. P. & Sucov, H. M. (2000) Fate of the mammalian cranial neural crest during tooth and mandibular morphogenesis. *Development* **127**, 1671–1679.

Cho, M. I. L. & Garant, P. R. (2000) Development and general structure of the periodontium. *Periodontology 2000* **24**, 9–27.

Coura, G. S., Garcez, R. C., de Aguiar, C. B., Alvarez-Silva, M., Magini, R. S. & Trentin, A. G. (2008) Human periodontal ligament: a niche of neural crest stem cells. *Journal of Periodontal Research* **43**, 531–536.

Duarte, W. R. (1998) cDNA cloning of S100 calcium-binding proteins from bovine periodontal ligament and their expression in oral tissues. *Journal of Dental Research* **77**, 1694–1699.

Fujita, T., Iwata, T., Shiba, H., Igarashi, A., Hirata, R., Takeda, K., Mizuno, N., Tsuji, K., Kawaguchi, H., Kato, Y. & Kurihara, H. (2007) Identification of marker genes distinguishing human periodontal ligament cells from human mesenchymal stem cells and human gingival fibroblasts. *Journal of Periodontal Research* **42**, 283–286.

Gay, I. C., Chen, S. & MacDougall, M. (2007) Isolation and characterization of multipotent human periodontal ligament stem cells. *Orthodontics and Craniofacial Research* **10**, 149–160.

Gronthos, S., Mrozik, K., Shi, S. & Bartold, P. M. (2006) Ovine periodontal ligament stem cells: isolation, characterization, and differentiation potential. *Calcified Tissue International* **79**, 310–317.

Hammarstrom, L., Heijl, L. & Gestrelius, S. (1997) Periodontal regeneration in a buccal dehiscence model in monkeys after application of enamel matrix proteins. *Journal of Clinical Periodontology* **24**, 669–677.

Han, X. & Amar, S. (2002) Identification of genes differentially expressed in cultured human periodontal ligament fibroblasts vs. human gingival fibroblasts by DNA microarray analysis. *Journal of Dental Research* **81**, 399–405.

Hoemann, C. D., El-Gabalawy, H. & McKee, M. D. (2009) In vitro osteogenesis assays: influence of the primary cell source on alkaline phosphatase activity and mineralization. *Pathologie et Biologie* **57**, 318–323.

Horiuchi, K., Amizuka, N., Takeshita, S., Takamatsu, H., Katsuura, M., Ozawa, H., Toyama, Y., Bonewald, L. F. & Kudo, A. (1999) Identification and characterization of a novel protein, periostin, with restricted expression to periosteum and periodontal ligament and increased expression by transforming growth factor beta. *Journal of Bone and Mineral Research* **14**, 1239–1249.

Iohara, K., Nakashima, M., Ito, M., Ishikawa, M., Nakasima, A. & Akamine, A. (2004) Dentin regeneration by dental pulp stem cell therapy with recombinant human bone morphogenetic protein 2. *Journal of Dental Research* **83**, 590–595.

Iohara, K., Zheng, L., Ito, M., Tomokiyo, A., Matsushita, K. & Nakashima, M. (2006) Side population cells isolated from porcine dental pulp tissue with self-renewal and multipotency for dentinogenesis, chondrogenesis, adipogenesis, and neurogenesis. *Stem Cells* **24**, 2493–2503.

Ishikawa, I., Iwata, T., Washio, K., Okano, T., Nagasawa, T., Iwasaki, K. & Ando, T. (2009) Cell sheet engineering and other novel cell-based approaches to periodontal regeneration. *Periodontology 2000* **51**, 220–238.

Itaya, T., Kagami, H., Okada, K., Yamawaki, A., Narita, Y., Inoue, M., Sumita, Y. & Ueda, M. (2009) Characteristic changes of periodontal ligament-derived cells during passage. *Journal of Periodontal Research* **44**, 425–433.

Iwata, T., Yamato, M., Tsuchioka, H., Takagi, R., Mukobata, S., Washio, K., Okano, T. & Ishikawa, I. (2009) Periodontal regeneration with multi-layered periodontal ligament-derived cell sheets in a canine model. *Biomaterials* **30**, 2716–2723.

Karring, T., Isidor, F., Nyman, S. & Lindhe, J. (1985) New attachment formation on teeth with a reduced but healthy periodontal ligament. *Journal of Clinical Periodontology* **12**, 51–60.

Lallier, T. E., Spencer, A. & Fowler, M. M. (2005) Transcript profiling of periodontal fibroblasts and osteoblasts. *Journal of Periodontology* **76**, 1044–1055.

Leucht, P., Kim, J. B., Amasha, R., James, A. W., Girod, S. & Helms, J. A. (2008) Embryonic origin and Hox status determine progenitor cell fate during adult bone regeneration. *Development* **135**, 2845–2854.

Lindroos, B., Maenpaa, K., Ylikomi, T., Oja, H., Suuronen, R. & Miettinen, S. (2008) Characterisation of human dental stem cells and buccal mucosa fibroblasts. *Biochemical and Biophysical Research Communications* **368**, 329–335.

Liu, Y., Zheng, Y., Ding, G., Fang, D., Zhang, C., Bartold, P. M., Gronthos, S., Shi, S. & Wang, S. (2008) Periodontal ligament stem cell-mediated treatment for periodontitis in miniature swine. *Stem Cells* **26**, 1065–1073.

Livak, K. J. & Schmittgen, T. D. (2001) Analysis of relative gene expression data using real-time quantitative PCR and the 2(T)(– Delta Delta C) method. *Methods* **25**, 402–408.

Matsubara, T., Suardita, K., Ishii, M., Sugiyama, M., Igarashi, A., Oda, R., Nishimura, M., Saito, M., Nakagawa, K., Yamanaka, K., Miyazaki, K., Shimizu, M., Bhawal, U. K., Tsuji, K., Nakamura, K. & Kato, Y. (2005) Alveolar bone marrow as a cell source for regenerative medicine: differences between alveolar and iliac bone marrow stromal cells. *Journal of Bone and Mineral Research* **20**, 399–409.

McCulloch, C. A. & Bordin, S. (1991) Role of fibroblast subpopulations in periodontal physiology and pathology. *Journal of Periodontal Research* **26**, 144–154.

Murakami, Y., Kojima, T., Nagasawa, T., Kobayashi, H. & Ishikawa, I. (2003) Novel isolation of alkaline phosphatase-positive subpopulation from periodontal ligament fibroblasts. *Journal of Periodontology* **74**, 780–786.

Nagatomo, K., Komaki, M., Sekiya, I., Sakaguchi, Y., Noguchi, K., Oda, S., Muneta, T. & Ishikawa, I. (2006) Stem cell properties of human periodontal ligament cells. *Journal of Periodontal Research* **41**, 303–310.

Nakahara, T., Nakamura, T., Kobayashi, E., Kuremoto, K., Matsuno, T., Tabata, Y., Eto, K. & Shimizu, Y. (2004) In situ tissue engineering of periodontal tissues by seeding with periodontal ligament-derived cells. *Tissue Engineering* **10**, 537–544.

Nakamura, S., Terashima, T., Yoshida, T., Iseki, S., Takano, Y., Ishikawa, I. & Shinomura, T. (2005) Identification of genes preferentially expressed in periodontal ligament: specific expression of a novel secreted protein, FDC-SP. *Biochemical and Biophysical Research Communications* **338**, 1197–1203.

Nimura, A., Muneta, T., Koga, H., Mochizuki, T., Suzuki, K., Makino, H., Umezawa, A. & Sekiya, I. (2008) Increased proliferation of human synovial mesenchymal stem cells with autologous human serum: comparisons with bone marrow mesenchymal stem cells and with fetal bovine serum. *Arthritis and Rheumatism* **58**, 501–510.

Nishida, E., Sasaki, T., Ishikawa, S. K., Kosaka, K., Aino, M., Noguchi, T., Teranaka, T., Shimizu, N. & Saito, M. (2007) Transcriptome database KK-periome for periodontal ligament development: expression profiles of the extracellular matrix genes. *Gene* **404**, 70–79.

Nyman, S., Karring, T., Lindhe, J. & Planten, S. (1980) Healing following implantation of periodontitis-affected roots into gingival connective tissue. *Journal of Clinical Periodontology* **7**, 394–401.

Nyman, S., Lindhe, J., Karring, T. & Rylander, H. (1982) New attachment following surgical treatment of human periodontal disease. *Journal of Clinical Periodontology* **9**, 290–296.

Pi, S. H., Lee, S. K., Hwang, Y. S., Choi, M. G. & Kim, E. C. (2007) Differential expression of periodontal ligament-specific markers and osteogenic differentiation in human papilloma virus 16-immortalized human gingival fibroblasts and periodontal ligament cells. *Journal of Periodontal Research* **42**, 104–113.

Peck, S. & Peck, L. (1993) A time for change of tooth numbering systems. *Journal of Dental Education* **57**, 643–647.

Ramakrishnan, P. R., Lin, W. L., Sodek, J. & Cho, M. I. (1995) Synthesis of noncollagenous extracellular matrix proteins during development of mineralized nodules by rat periodontal ligament cells in vitro. *Calcified Tissue International* **57**, 52–59.

Sakaguchi, Y., Sekiya, I., Yagishita, K. & Muneta, T. (2005) Comparison of human stem cells derived from various mesenchymal tissues: superiority of synovium as a cell source. *Arthritis and Rheumatism* **52**, 2521–2529.

Sculean, A., Nikolidakis, D. & Schwarz, F. (2008) Regeneration of periodontal tissues: combinations of barrier membranes and grafting materials – biological foundation and preclinical evidence: a systematic review. *Journal of Clinical Periodontology* **35**, 106–116.

Sekiya, I., Larson, B. L., Smith, J. R., Pochampally, R., Cui, J. G. & Prockop, D. J. (2002) Expansion of human adult stem cells from bone marrow stroma: conditions that maximize the yields of early progenitors and evaluate their quality. *Stem Cells* **20**, 530–541.

Seo, B. M., Miura, M., Gronthos, S., Bartold, P. M., Batouli, S., Brahim, J., Young, M., Robey, P. G., Wang, C. Y. & Shi, S. (2004) Investigation of multipotent postnatal stem cells from human periodontal ligament. *Lancet* **364**, 149–155.

Somerman, M. J., Archer, S. Y., Imm, G. R. & Foster, R. A. (1988) A comparative study of human

periodontal ligament cells and gingival fibroblasts in vitro. *Journal of Dental Research* **67**, 66–70.

Sonoyama, W., Liu, Y., Fang, D., Yamaza, T., Seo, B. M., Zhang, C., Liu, H., Gronthos, S., Wang, C. Y., Shi, S. & Wang, S. (2006) Mesenchymal stem cell-mediated functional tooth regeneration in swine. *PLoS One* **1**, e79.

Sotiropoulou, P. A., Perez, S. A., Salagianni, M., Baxevanis, C. N. & Papamichail, M. (2006) Characterization of the optimal culture conditions for clinical scale production of human mesenchymal stem cells. *Stem Cells* **24**, 462–471.

Trubiani, O., Di Primio, R., Traini, T., Pizzicannella, J., Scarano, A., Piattelli, A. & Caputi, S. (2005) Morphological and cytofluorimetric analysis of adult mesenchymal stem cells expanded ex vivo from periodontal ligament. *International Journal of Immunopathology and Pharmacology* **18**, 213–221.

Wada, N., Menicanin, D., Shi, S., Bartold, P. M. & Gronthos, S. (2009) Immunomodulatory properties of human periodontal ligament stem cells. *Journal of Cell Physiology* **219**, 667–676.

Wang, H. L., Greenwell, H., Fiorellini, J., Giannobile, W., Offenbacher, S., Salkin, L., Townsend, C., Sheridan, P. & Genco, R. J. (2005) Periodontal regeneration. *Journal of Periodontology* **76**, 1601–1622.

Xu, J., Wang, W., Kapila, Y., Lotz, J. & Kapila, S. (2009) Multiple differentiation capacity of STRO-1+/CD146+PDL mesenchymal progenitor cells. *Stem Cells and Development* **18**, 487–496.

Yamada, S., Murakami, S., Matoba, R., Ozawa, Y., Yokokoji, T., Nakahira, Y., Ikezawa, K., Takayama, S., Matsubara, K. & Okada, H. (2001) Expression profile of active genes in human periodontal ligament and isolation of PLAP-1, a novel SLRP family gene. *Gene* **275**, 279–286.

Zhou, Y., Hutmacher, D. W., Sae-Lim, V., Zhou, Z., Woodruff, M. & Lim, T. M. (2008) Osteogenic and adipogenic induction potential of human periodontal cells. *Journal of Periodontology* **79**, 525–534.

Address:
Teruo Okano
Institute of Advanced Biomedical Engineering and Science
Tokyo Women's Medical University
8-1 Kawada-cho
Shinjuku-ku
Tokyo 162-8666
Japan
E-mail: tokano@abmes.twmu.ac.jp

Clinical Relevance

Scientific rationale for the study: Cytotherapy using PDL cells has proven to be effective. However, there is no standard protocol for the culture of human PDL cells. In this study, we validated the culture conditions and characteristics of human PDL cells for human clinical trials. *Principal findings*: Human PDL cells were successfully extracted with collagenase/dispase and exhibited high proliferative capacity, high ALP activity, and multi-potency. Some genes (NCAM1, S100A4, and periostin) were preferentially expressed in human PDL cells and can be useful markers for the identification of human PDL cells. *Practical implications*: Human PDL cells could be a promising source of cells for regenerative medicine.